Sekudewicz, I., Syczewski, M. D., Rohovec, J., Matoušková, Š., Kowalewska, U., Blukis, R., Geibert, W., Stimac, I., Gąsiorowski, M. (2024): Geochemical behavior of heavy metals and radionuclides in a pit lake affected by acid mine drainage (AMD) in the Muskau Arch (Poland). - Science of the Total Environment, 908, 168245.

https://doi.org/10.1016/j.scitotenv.2023.168245

Geochemical behavior of heavy metals and radionuclides in a pit lake affected by acid mine drainage (AMD) in the Muskau Arch (Poland)

Ilona Sekudewicz[1], Marcin Syczewski[2], Jan Rohovec[3], Šárka Matoušková[3], Urszula Kowalewska[1], Roberts Blukis[2,4], Ingrid Stimac[5], Michał Gąsiorowski[1]

[1]Institute of Geological Sciences, Polish Academy of Sciences, 00818 Warszawa, Twarda 51/55, Poland

[2] Helmholtz Centre Potsdam, GFZ German Research Centre for Geosciences, Telegrafenberg, Potsdam D-14473, Germany [3]Institute of Geology, Czech Academy of Sciences, 16500 Praha, Rozvojová 269, Czech Republic

[4]Leibniz-Institut für Kristallzüchtung, Max-Born-Str. 2, 12489 Berlin, Germany

[5]Alfred Wegener Institute for Polar and Marine Research, Marine Geochemistry, 27570 Bremerhaven, Germany

Corresponding author: Ilona Sekudewicz; i.sekudewicz@twarda.pan.pl

ORCID number of the corresponding author: 0000-0003-4525-8200

Abstract:

Pit lakes of the 'anthropogenic lake district' in the Muskau Arch, located along the Polish-German border (central Europe), are strongly affected by acid mine drainage (AMD). The studied acidic pit lake ŁK-61 (pH <3), originated from lignite mining ended in 1980s, can be also exposed to the floods due to its location in the flood hazard area. The key factors responsible for the distribution of selected heavy metals (e.g., Cr, Cu, Ni, Pb, Zn) and radioactive isotopes (^{137}Cs and ^{210}Po) in the bottom sediments of ŁK-61 Lake are Fe and Al secondary minerals crystallization and sorption onto authigenic and allogenic phases. These processes might be driven by lake inflow, which is an important source of dissolved elements and probably also solid particles. During episodic depositional events (such as floods and heavy rainfalls), the physiochemical parameters of the lake water of ŁK-61 Lake was changed, as documented by summer 2010 Nysa Łużycka River flood. The flood likely caused an increase in the water pH, which is interpreted from diatom studies. The down-core profiles of heavy metals and radionuclides (HMR) were probably affected by this flood event, what in addition prevent age determination of the collected lake sediments by using ^{137}Cs and ^{210}Pb dating techniques. On the other hand ^{137}Cs and ^{210}Po enriched sediment layer can serve as an useful chronostratigraphic marker. Geochemical modeling showed that flood related shift in physicochemical conditions in ŁK-61 Lake could have led to the crystallization of fresh precipitates that captured and immobilized dissolved solids. Moreover, contaminated particles with HMR could have also been delivered by incoming waters, along with nutrients, such as phosphorus and nitrogen.

Highlights:

- Understanding present and past sedimentation conditions in acidic pit lake
- Pollutants delivered to the lake from the catchment area and possibly by the river
- Diatom inferred pH of the lake water may indicate flood event
- Radionuclides ^{137}Cs and ^{210}Po as fingerprints of depositional events
- C/N ratio indicate the supply of allochthonous organic matter during a flood

Keywords: Lignite; Radiocesium, Polonium, Lake sediments, Flood; Anthropocene

Graphical abstract:

1. Introduction

Factors controlling the distribution of heavy metals in natural environments affected by acid mine drainage (AMD) has been widely studied (e.g., Cánovas et al., 2007; Friese, 2004; Hierro et al., 2014; Lee et al., 2002; Torres et al., 2013). However, the geochemical behavior of radionuclides in such ecosystems is still far from being understood (Blasco et al., 2016). Most of the studies regarding radioisotopes in AMD-affected aquatic ecosystems mainly concerned uranium (e.g., Barbero et al., 2014; Hierro et al., 2012; Manjón et al., 2019; Villa et al., 2011; Yamamoto et al., 2010). However, to our knowledge, only a few studies have focused on the distribution of cesium ^{137}Cs, lead ^{210}Pb, or polonium ^{210}Po in water reservoirs affected by AMD (Abril et al., 2018; Blasco et al., 2016; Mantero et al., 2020; Thomas et al., 2020, 2022). Nevertheless, understanding of the mechanisms responsible for the cycling of these particular radioactive isotopes in lake ecosystems is crucial because they are useful tools for dating sediments, as well as because they can also pose a dangerous threat to biota (Abril et al., 2018; Aközcan et al., 2018; Appleby, 2005; Edgington et al., 1991; Swarzenski, 2014). In addition, they might be important tracers of depositional events in the water reservoirs, even if they cannot provide an unambiguous, accurate chronology for the sediment record (e.g., Abril et al., 2018; Mabit et al., 2014; Zapata and Nguyen, 2009).

Polonium ^{210}Po (half-life = 138.38 days) is a naturally occurring radioactive isotope that in rocks, deep soils and sediments is expected to be in a secular equilibrium with its indirect parent isotopes, radium ^{226}Ra (half-life = 1622 years) and 'supported' lead ^{210}Pb (half-life = 22.23 years) (Carvalho et al., 2017; Cook et al., 2018; Persson and Holm, 2011). In younger sediments (<100 y), ^{210}Po is associated with its progenitor, so-called 'unsupported' or 'excess' ^{210}Pb, of which dominant sources in the lacustrine ecosystems are atmospheric deposition and surface runoff (e.g., Swarzenski, 2015; Zapata and Nguyen, 2009). Therefore, ^{210}Po is commonly used to indirectly determine ^{210}Pb activity concentrations in the sediments assuming they are in a secular equilibrium (e.g., Matthews et al., 2007; Zaborska et al., 2007). For this reason, a down-core profile of ^{210}Po is supposed to follow the exponential curve (in accordance with the law of radioactive decay), provided the constant flux of excess ^{210}Pb, undisturbed sedimentation conditions and lack of post depositional processes that might cause redistribution of deposited $^{210}Pb_{ex}$ (Appleby, 2005; Appleby and Oldfield, 1978; Swarzenski, 2014).

Radiocesium ^{137}Cs (half-life = 30.07 years) is an anthropogenic radioactive isotope, which was released into the natural environment as a result of nuclear weapons tests and nuclear power plant accidents in Chernobyl (1986) and Fukushima (2011) (Appleby, 2005; Ashraf et al., 2014; Smith and Beresford, 2005). Subsequently, ^{137}Cs was deposited at the bottom of the

water reservoirs as a consequence of atmospheric fallout and radiocesium-bearing particles input at a later stage (Ashraf et al., 2014; Smith et al., 2005). Assuming undisturbed sedimentation conditions, a characteristic peak of increased content of this radioisotope can be observed in a down-core profile of ^{137}Cs (e.g., Appleby, 2005). Hence, ^{137}Cs is widely regarded as an important chronostratigraphic marker and commonly used to validate chronologies based on other methods, such as ^{210}Pb (Abril et al., 2018; Appleby, 2008; Baskaran et al., 2014; Putyrskaya et al., 2015).

The distribution of heave metals and radionuclides (HMR) in AMD-affected pit lakes can be controlled by several factors, such as specific limnological properties, the age of the lake and degree of its neutralization/eutrophication, mineralogical composition of rocks forming the embankments and catchment area (Blasco et al., 2016; Boehrer, 2013; Friese et al., 1998; Gąsiorowski et al., 2021; Geller et al., 2013; Sánchez España et al., 2008; Schultze, 2013; and others). Moreover, there are many factors that can alter the vertical distribution of HMR in sediment profiles, such as physical mixing caused by wind-wave action and bioturbations, as well as chemical remobilization (e.g., Abril et al., 2018; Appleby, 2005; Baskaran et al., 2014; Klaminder et al., 2012; Putyrskaya et al., 2015). Moreover, some depositional events, such as heavy rainfalls or floods, can also disrupt the processes responsible for the distribution of these elements in AMD-affected reservoirs (e.g., Abril et al., 2018; Cánovas et al., 2007; Guerrero et al., 2021; Herzsprung et al., 2010; Mayes et al., 2021). Such events can cause a change in water pH and redox conditions, which are considered the main parameters determining the behavior of trace metals and radionuclides in such ecosystems (e.g., Hierro et al., 2014; Shi et al., 2021). An increase in water pH can lead, for example, to the precipitation of secondary minerals, which can capture dissolved metals by co-precipitation/precipitation and/or sorption processes (e.g., Alpers et al., 1994; Azzali et al., 2014; Hierro et al., 2014). A subsequent decrease in water pH may lead to dissolution of pH-sensitive mineral phases and simultaneous release of immobilized elements (e.g., Mayes et al., 2021; Wisotzky, 1998). Moreover, floods can carry large amounts of particles and dissolved solids, what can also significantly affect the distribution of HMR in the bottom sediments of pit lakes (e.g., Appleby, 2005; Herzsprung et al., 2010; Mayes et al., 2021; Torres et al., 2013; Walling and Quine, 1993). Incoming river waters can also transport significant amounts of nutrients, such as phosphorus (P), as observed in the case of Goitsche Lake in Germany (Herzsprung et al., 2010). The input of nutrients (P and nitrogen (N)) affects the growth of microorganisms (e.g., diatoms) and indirectly alters the geochemical behavior of other elements in the reservoirs (e.g., Kleeberg and Grüneberg, 2005; Paulsson and Widerlund, 2021; Schultze, 2013).

The studied ŁK-61 Lake is a pit lake in the Muskau Arch (western Poland) affected by AMD (formed as a result of the oxidation and dissolution of iron sulfides), which can be especially stricken by depositional events due to its location at the flood hazard area (Fig. 1). The main objective of the presented research was to investigate the key processes responsible for the cycling of selected heavy metals (e.g. Cr, Cu, Ni, Pb, Zn) and radionuclides (^{137}Cs and ^{210}Po) in the studied lake. The impact of potential depositional events on the distribution of selected trace metals and radioisotopes in the bottom sediments of ŁK-61 and on their dating using the ^{137}Cs and ^{210}Pb methods were also discussed. In order to achieve the intended goals, the physicochemical parameters and the elemental composition of tributary and lake water, as well as the content of HMR in lake sediments of ŁK-61 were measured. Based on the analysis of subfossil diatoms, the former pH of lake water was reconstructed. In order to discover the sedimentation conditions and to identify past depositional events, the grain size distribution, concentrations of ^{40}K activity, and mineralogical composition of selected samples of lake sediments were also examined. Additionally, to characterize the origin of organic matter (OM) in the collected lake sediments, C/N ratio was also determined on the basis of elemental analysis.

2. Sampling and methods

2.1. Study area

The study area is located in the Muskau Arch (also known as Łuk Mużakowa and Muskauer Faltenbogen) in Lubusz Voivodeship (western Poland) near the Polish-German border (Fig. 1). The Muskau Arch is an arch-shaped glaciotectonic terminal moraine formed during the Last Glacial Period (Bożęcki, 2013). It covers an area of about 250 km^2, of which about 80 km^2 is located in Poland. Natural resources mined in this area were brown coal, clays, sand and gravel (Gruszecki et al., 2006). There are about 100 lakes, most of which were created as a result of lignite mining from the 19th century to the 1970s (Kupetz, 1997; Lutyńska and Labus, 2015). The exploitation of lignite lasted until 1973, when the 'Babina' mine located east of Łęknica was closed down (Koźma and Kupetz, 2008). Clay mining in this area continued until the 1990s (Gruszecki et al., 2006). Therefore, the greatest anthropogenic changes in the natural environment can be observed in the area of Łęknica (Solski et al. 1988).

The study site was ŁK-61 Lake (51°31'31.746"N, 14°45'19.824"E; also known as 'Hydro' or 'Staw Południowy' Lake) located near to Łęknica, in close proximity to the Polish-German border (Fig. 1). The area of the lake is 2.71 ha and its maximum depth is 7.5 m. It has one tributary, which is a stream flowing into the lake on its northern side. The regional geology

of the study area is characterized by sands and gravels of the alluvial terrace (Fig. 2) (Bartczak and Gancarz, 1998). To the north of the lake, there are sands, silts, kaolinite clays, clays, and brown coal. ŁK-61 is a pit lake located on the site of an open-pit lignite mine that was operated from 1957 to the 1970s (Koźma, 2009). There were also refractory clay mines on the northern side of the lake, which were closed down in the 1990s (Gruszecki et al., 2006). Nowadays, the study area is located in a landscape park and it is surrounded by deciduous and mixed coniferous forests.

The studied lake is situated a short distance (approx. 200 m) from the Nysa Łużycka River (Lausitzer Neiße) (Fig. 1). It is located in a flood hazard area, where the probability of flooding is 10% (once per 10 years) (PGW WP, 2021). The last of floods recorded in this area was the flood that occurred in the first days of August 2010 (MKOO, 2010). Previously, the highest water level of the Nysa Łużycka River was recorded on the stream gauge (Przewóz) located near the study area in 1981.

2.2. Sampling and sample preparation

The fieldwork was carried out in September 2020 and 2021. The depth of the lake bottom was measured in two transects with a portable echo sounder Echotest II. Physicochemical parameters of water (temperature, pH, redox potential (Eh), electrical conductivity (EC), and dissolved oxygen (DO)) were measured in situ with a multi-parameter portable Multi 3620 IDS SET G meter manufactured by WTW during sampling in September 2020 (site no. WA) and 2021 (site no. WB). Samples from the tributary (sites no. T 1-3) and water column (WA) were collected in September 2020 (Fig. 1). Samples of lake water (site no. WA 1-7) were collected every 1 m from the top layer to the bottom of the water column using a vertical sampler with a capacity of 5 L. Each water sample was then filtered through a CA filter (0.45 µm pore size), preserved with double-distilled HCl (35%), and stored in 50 mL polyethylene bottles at 4 °C until analyzed. The lake sediment column (C1) was collected in September 2020 at the deepest point of the lake bottom using a UWITEC gravity core with a polycarbonate pipe (inner diameter 90 mm) (Fig. 1). The core (length 55 cm) was divided in the field into 1 cm slices and stored in PET containers at 4 °C. The samples were then transported to the laboratory, dried at 65 °C, ground, and homogenized for further analysis. A portion of each sample was left unground for particle size analysis.

2.3. Tributary and lake water samples

2.3.1. Elemental composition and DOC content

The concentrations of macroelements in water samples were determined with the ICP-EOS (Agilent 5100) at the Institute of Geology of the Czech Academy of Sciences (CAS) in

Prague. Alkali metals (Na 589.6 nm, K 766.5 nm, Mg 279.6 nm, Ca 317.9 nm) and other macroelements (Al 396.2 nm, Fe 259.9 nm, Mn 257.6 nm, P 213.6 nm, S 182.0 nm, Si 212.4 nm) were quantified with radial and axial plasma settings, respectively. Mixed standards for the instrument calibration were prepared from commercially available single-element SRM (Analytika spol. s.r.o). QC/QA procedure was based on the ERM CA 615 CRM, producing results within the certificate range (Fe, Mn) and with recoveries 97-102 % (Ca, Mg, K, Na).

Trace elements in water samples were quantified using high-resolution sector-field ICP-MS Element II (Thermo Fisher Scientific) at the Institute of Geology CAS. The instrument was tuned using a homemade multi-element standard to achieve the highest sensitivity of ^{115}In and ^{238}U, balanced stability and oxide formation below 8%. Instrumental calibration was performed with a multi-element calibration solution prepared from commercially available single-element standards (CPA Chem). The isotope ^{115}In was used as an internal standard to correct for the instrumental and plasma drift. Quantification was performed in low resolution (LR) and in medium resolution (MR).

Chlorides were quantified by HPLC at the Institute of Geology CAS. Aqueous carbonate/hydrogen carbonate buffer (3.5 mmol/L) was used as the mobile phase. A Star Ion A300 anion exchange column (Phenomenex) and a CDD-10 Avp conductivity detector (Shimadzu) were used for separation and detection. The system was calibrated with a mixed standard solution CRM (Analytika spol. s.r.o.). QC/QA procedure was based on the CRM ERM CA 615. Dissolved organic carbon (DOC) was determined at the Institute of Geology CAS using the combustion catalytic infrared method on the Shimadzu TOC-V CPH. A basic standard solution was prepared using oxalic acid dihydrate. Concentrations of DOC in water samples were determined in triplicate and 2 additional determinations were performed if the RSD was >5 %. The stability of the measurements was monitored by analyzing the dihydrogen phthalate solution after every 5 samples.

2.4. Lake sediment samples

2.4.1. Grain size and elemental analyses

The lake sediment samples were dispersed with KOH, and then carbonates were removed with HCl and OM was destroyed with H_2O_2 and HNO_3, prior to grain size analysis. The particle size distribution of the sediment samples was determined using sieve analysis (for particles >1000 μm) and a laser particle size analyzer (CILAS 1190) at the Institute of Geology CAS. The analyses were performed in the wet dispersion mode in the device range from 0.04 to 1000 μm. Classification of lake sediments in terms of particle size was carried out using the

Shepard sediment classification diagram (Shepard, 1954) and the 'ggtern' R package (Hamilton and Ferry, 2018).

The analysis of the content of total organic carbon (TOC) and total nitrogen (TN) in the lake sediments was performed using the Vario CUBE elemental analyzer at the Institute of Geological Sciences of the Polish Academy of Sciences (ING PAN) in Warsaw. A small portion (5-6 mg) of each sample was transferred to tin capsules and burned at 1150 °C. Then, CO_2 and N_2 gases were separated in a chromatography column and measured with a thermal conductivity detector. Sulfanilic acid was used as the standard to validate the analyses. The measurement uncertainty for TOC and TN was 0.6%, and 0.18%, respectively.

2.4.2. Alpha and gamma spectroscopy

The radiochemical separation of ^{210}Po from the lake sediment samples was carried out according to the modified procedure presented by Flynn (1968). Sediment samples (approximately 0.6 g) were spiked with $^{208+209}$Po and digested on a hot plate with HCl (35%) and HNO_3 (65%). The organic components were destroyed in the samples by heating with HNO_3 (65%) and H_2O_2 (32%) (Jia et al., 2004; Matthews et al., 2007). Finally, polonium isotopes were spontaneously deposited (ion exchange reaction) onto silver discs in 0.5 M HCl (Martin and Blanchard, 1969). Sodium citrate and hydroxylamine hydrochloride were added to the solution prior the deposition process to prevent the deposition of competing ions (e.g. Fe^{3+}) (Flynn, 1968; Jia et al., 2004). The chemical recovery for ^{210}Po ranged from 40 to 60%. The activity concentrations of ^{208}Po, ^{209}Po and ^{210}Po were measured using an Octete (Ortec) alpha spectrometer at the ING PAN in Warsaw. Samples were counted for about 72 h. The average (arithmetic mean; n = 33) uncertainty of ^{210}Po activity concentration measurements was 1.5 Bq kg^{-1} (3%).

The concentrations of ^{137}Cs and ^{40}K activity in the lake sediments were measured using a low background gamma spectrometer (Canberra-Packard) with a Broad Energy Germanium (BE5030) detector (FWHM = 1.05 keV at 661.7 keV for ^{137}Cs and 1.65 keV at 1460.8 keV for ^{40}K) at the ING PAN in Warsaw. In order to verify the quality of the measurements, the reference material of lake sediments (IAEA-SL-2) was analyzed. All samples (from 1 to 10 g dry weight) were analyzed in a flat cylinder geometry. The Genie 2000 software was used for data acquisition. Sample counting time ranged from 48 to 78 h. All obtained values were converted to the sampling date (September 24, 2020). The minimum detectable activity (MDA) for ^{137}Cs and ^{40}K was 0.7 Bq kg^{-1} and 13.5 Bq kg^{-1}, respectively. The uncertainty of the measurements of ^{137}Cs and ^{40}K activity concentrations varied from 22 to 39% and from 9 to 23%, respectively.

2.4.3. ICP-OES analysis

Selected lake sediments samples were digested in one batch consisting of 17 samples, 4 procedural blanks, and 3 reference material samples. The certified reference material was a marine sediment (NRC-MESS-4). Approximately 75 mg of each sediment sample was transferred to PTFE vials and digested with double-distilled HNO_3 (65%), HCl (32%), and HF (X%) using the microwave digestion system MARS 6 (CEM Corporation, USA) at the Alfred Wegener Institute Helmholtz Centre for Polar and Marine Research in Bremerhaven. All samples were then appropriately diluted with double-distilled 1.5 M HNO_3 prior to analysis. The concentrations of selected elements in the prepared samples were measured in triplicates using the ICP-OES (iCAP 7000 Series; Thermo Scientific) (Table S2; Supplementary Materials). Single-element standard solutions (Roti®Star, CarlRoth GmbH) were used to perform external calibration for quantitative analysis. Yttrium was added as an internal standard to correct the results for instrumental drift. The relative standard deviation (RSD) for all analyses was less than 5% (Table S3; Supplementary Materials). The limit of detection (LOD) and limit of quantification (LOQ) for the measured elements are presented in Table S4 (Supplementary Materials).

2.4.4. Mineralogical analyses

Mineralogical analyses of selected samples of lake sediments were performed at the Helmholtz Centre Potsdam, GFZ German Research Centre for Geosciences. X-ray diffraction measurements were performed with a STOE STADI P diffractometer with an Ag X-ray source fitted with a curved Ge (111) monochromator and two DECTRIS MYTHEN2 detectors in a flat plate transmission geometry. Diffraction patterns were measured over a range of 0 – 73 degrees 2Θ (Q = 0 – 13.3 Å-1) for a duration of 3 h per data point. Rietveld refinements were performed using GSAS-II software (Toby and Von Dreele, 2013). Reference CIF files were obtained from AMCSD database and were refined for unit cell, grain size and microstrain, sheet silicates also for preferential orientation. Background was approximated using Chebyshev polynomials and the instrument function was calibrated by empirically fitting Caglioti function with included asymmetry to an LaB6 standard measured in the same geometry.

Infrared absorption (IR) spectra were measured with a ThermoFisher Nicolet iS5 FT-IR spectrometer equipped with an iD7 single reflection diamond ATR accessory and KBr optics. For each sample, 32 spectra with a resolution of 4 cm^{-1}, were averaged. The spectra shown here are presented without ATR corrections and therefore may not match the exact peak intensity and wavenumber values measured in transmission from other studies. Reference spectra for

montmorillonite, kaolinite and ferrihydrite were measured in our lab with the same settings as the samples while the other IR reference spectra were taken from the RRUFF database.

The scanning electron microscopy coupled with energy dispersive spectroscopy (SEM-EDS) of selected samples was preformed using FEI Quanta 3D FEG Dual Beam (SEM) and EDAX Octane elect plus. Electron microscope was operating at 20 kV, 4nA. Before measurements samples were placed on 10 mm aluminum pin stubs and coated with 20 nm of C using vacuum coater (LEICA EM ACE600).

2.4.5. Diatom analysis and DI-pH modeling

For diatom analysis, 55 samples were collected every centimeter. Slides were prepared according to the standard method described by Battarbee (1986). In order to oxidize the OM, one cubic cm of each sample was heated with 30% hydrogen peroxide (H_20_2). The sediments were then washed three times with distilled water and diluted to 20-100 ml. Permanent slides were mounted with Naphrax (R.I. = 1.75). An Olympus BX40 light microscope with a ×100 oil immersion objective was used to identify and count diatom valves. Diatom identification was based on Krammer and Lange-Bertalot (1986, 1988, 1991a, 1991b), Lange-Bertalot and Metzeltin (1996), Krammer (2000) and Lange-Bertalot et al. (2017). The reconstruction of lake water pH (DI-pH) was carried out using the C2 software version 1.8 (Juggins 2001). It was performed with the pH training datasets created for post-mining lakes in the Muskau Arch (Sienkiewicz and Gąsiorowski 2017). The best squared correlation between inferred and observed values (R2) values and the lowest root mean squared error for the training set (apparent RMSE) of the pH model were obtained using the weighted averaging method with reduced weight of species with a high pH tolerance, together with the inverse deshrinking (WATOL_Inv).

2.5. Data analysis

Statistical analyses were performed using R 4.0.4 (R Core Team, 2021). The statistical distribution of the data was determined using the Shapiro-Wilk test. Most of the data were non-normally distributed, therefore spearman's rank correlation coefficients (p-value <0.05) were calculated to determine the relationship between selected variables with the R package 'Hmisc' (Frank and Harrell, 2023). Geochemical modeling was performed using the Gechemist's WorkBench® software (Bethke, 1996). The database used in this study was a modified GWB's thermo-minteq database.

3. Results

3.1. Surface and lake water

The physicochemical parameters and elemental composition of the tributary and lake water are presented in Table 1 and Table S1 (Supplementary Materials), respectively. Physicochemical parameters measured in the upper layer of the water column in September 2020 and 2021 did not differ significantly (Table 1). These values were also relatively similar to those measured in the tributary (T 1-3) (Table 1; Table S1). The obtained results showed that ŁK-61 is a stratified lake with a chemocline occurring between the depth of 5.5 and 6.5 m of the water column (Fig. 3). The surface layer (epilimnion) of the water column was characterized by low pH (pH = 2.9) and high mineralization values (EC >1900 µS cm^{-1}). In the bottom zone (hypolimnion), the content of DO (<2 mg L^{-1}) decreased significantly, while the values of pH (>5), EC (>2700 µS cm^{-1}), and the content of DOC (>32 mg L^{-1}) increased. An increase in the content of Fe, S, K and Na, as well as a decrease in the content of Al, Ca, Mg, Mn and Si in the hypolimnion of ŁK-61 was also observed (Fig. 3; Table S1).

3.2. Lake sediments

3.2.1. Organic matter (OM) content and grain-size distribution

The average content of TOC in the collected sediment profile was 3.8% (arithmetic mean; n = 55). The vertical distribution of TOC content was rather constant along the entire length of the sediment column (Fig. 4). The highest TOC content (above 5%) was found at depths of 20 - 21 cm and 41 cm of the core. The TN content was below the limit of detection in most of the collected lake sediments, with the exception of samples located at depths of 1 - 3 cm and 7 - 10 cm (Fig. 4). The content of TN in these samples ranged from 0.19 to 0.3%. Only for these samples it was possible to calculate the C/N ratio, which ranged from 18 to 26.

The average water content and wet bulk density of the collected sediment column were 57% and 1.5 g cm^{-3} (arithmetic mean; n = 55), respectively. The vertical distribution of the wet bulk density of lake sediments was variable in the entire length of the core (Fig. 4). The highest values of the wet bulk density (above 1.7 g cm^{-3}) were observed in the case of samples collected the depths of 6, 18, 21, 27 - 28, 32, 42 cm of the core. Based on Sheppard's classification diagram, lake sediment samples were classified as clayey silt and silty clay (Shepard, 1954). The average content of clay, silt, and sand fractions in the collected sediment column was 44.8, 54.9, and 0.3 % (arithmetic mean; n = 27), respectively. The highest content of the clay fraction (above 50%) was found in the samples collected from the depths of 13 - 18 and 38 cm of the core. In turn, increased content of the silt fraction (above 60%) was detected in the samples located at the depths of 1, 7, 22, 28, and 40 - 42 cm of the core. The highest content of the silt fraction was measured in a sample from a depth of 7 cm (68%). A significant increase in the

content of the sand fraction was observed in samples taken from depths of 40 cm (2.9%) and 54 cm (2.8%) of the core.

3.2.2. Radionuclides distribution

The average content of ^{210}Po in the collected sediment column was 45.2 ± 1.5 Bq kg^{-1} (arithmetic mean; n = 33). The vertical distribution of ^{210}Po activity concentrations in the collected core was irregular and did not follow a trend of the theoretical distribution of unsupported ^{210}Pb (assuming isotopic equilibrium), which decays exponentially with time, according to the law of radioactive decay (Appleby, 2005; Swarzenski, 2015). The peak of ^{210}Po content was observed in samples collected at the depths of <3 and 7 - 11 cm of the core (Fig. 4). The maximum concentration of ^{210}Po activity was registered in a sample collected at a depth of 10 cm (90.1 ± 3.1 Bq kg^{-1}). A moderate positive correlation was observed between the content of ^{210}Po and Mn (R_s = 0.53), P (R_s = 0.56), Sr (R_s = 0.50), Zn (R_s = 0.52), and TN (R_s = 0.52) (Table S5).

The vertical distribution of ^{137}Cs activity concentrations in the collected sediment column was irregular mostly in its upper part (Fig. 4). In a significant number of samples, the concentration of ^{137}Cs activity was below the limit of detection. A significant peak of ^{137}Cs content was found at the depths of 7 - 11 cm (up to 9.4 ± 2.0 Bq kg^{-1}), as in the case of ^{210}Po. A slight increase in ^{137}Cs activity concentration was also noted at the depth of 34 cm (1.9 ± 0.4 Bq kg^{-1}) and >50 cm (2.1 ± 0.5 Bq kg^{-1}) of the core. A moderate positive correlation was observed between the content of ^{137}Cs and Mg (R_s = 0.75), Ni (R_s = 0.80), Pb (R_s = 0.74), and Sr (R_s = 0.76) (Table S5).

The content of ^{40}K measured in the collected sediment column showed a different vertical distribution than that of ^{210}Po and ^{137}Cs (Fig. 4). The average concentration of ^{40}K activity in the core was 426.7 ± 43.6 Bq kg^{-1} (arithmetic mean; n = 26). A significant decrease in the content of this radioisotope was noticed in samples collected at the depths of 3, 7, 13 and 48 cm (Fig. 4). A significant increase in the content of ^{40}K was registered in samples collected at the depths of 5, 9-10, 22, 38 - 40, and >50 cm. A strong positive correlation was observed between the content of this radionuclide and Ba (R_s = 0.92), K (R_s = 0.94), Na (R_s = 0.89), and moderate with Cu (R_s = 0.71) (Table S5). Moreover, a strong negative correlation was found between the content of ^{40}K and Fe (R_s = -0.84).

3.2.3. Elemental composition

The elemental composition of selected lake sediment samples is presented in Fig. 4 and Table S1 (Supplementary Materials). The presented vertical distributions of concentrations of selected elements in the core were normalized to Al, considering the dominant alumina-silicate

minerals in the catchment area (Loring, 1991). Based on the obtained results, it can be observed that the vertical distribution of the content of almost all elements was significantly disturbed in the upper part of the sediment column (Fig. 4). The concentration of most elements (Na, Mg, P, Cu, Ni, Pb, Zn, etc.) was significantly increased between 7 and 12 cm of core depth. The content of Al and Ti was increased at the depths of 9 - 16 cm and 12 - 16 cm, respectively. Moreover, the content of Al, Ti, and K, was slightly increased in the samples located at the depths of 5 cm and >25 cm of the core. Fe concentration was significantly increased in the upper part of the sediment column (up to 3 cm depth) and at depths of 7, 16 - 20, and 45 cm. Similarly, the S content was elevated at the top (2-3 cm depth) of the core and slightly also at the depth of 7 cm. A slightly different vertical distribution, in comparison to above mentioned elements, was observed in the case of Ca and Mn, where the concentration of these elements was elevated in samples collected at the depths of 1, 3, 7 - 10, and 16 cm of the core.

Fe content in collected lake sediments was strongly positively correlated with S (R_s = 0.84) and Ca (R_s = 0.8) (Table S5). These elements (especially Fe) were significantly negatively correlated with Ba, K, Ti, and ^{40}K. Ca content in selected sediment samples was also strongly positively correlated with Mn (Rs = 0.85) and TN (Rs = 0.81). Al content was strongly positively correlated with Cr, Li, Mg, Ni, Pb, Ti, as well as strongly negatively correlated with TOC. ^{210}Po and ^{137}Cs were moderately positively correlated with Mn, P, Sr, Zn, and TN, and Cr, Mg, Ni, P, Pb, Sr, and Zn, respectively.

3.2.4. Mineralogical composition

Quantitative mineralogical analyses using a Rietveld refinement were performed only for selected samples of lake sediments collected from the core of ŁK-61 Lake. Due to a very fine grained or amorphous nature of a significant fraction of the samples, the Rietveld refinement could not be performed to a very high quality and accuracy. XRD analyses showed that lake sediments of ŁK-61 consist mostly of quartz, kaolinite and phyllosilicate minerals (possibly muscovite, illite or smectite group) (Fig. 5). IR analyses showed that the selected samples of lake sediments did not differ significantly from each other (Fig. 6, A). Significant amount of ferrihydrite and some carbonates were present in the studied samples (e.g. in a sample collected from a depth of 10 cm of the core), however, these could not be reliably quantified from the IR data (Fig. 6, B). The amount of ferrihydrite is similar in all lake sediment samples though. Qualitatively the samples displayed very strong fluorescence in Cu-XRD (which is why the analysis was performed using Ag-XRD) indicating a high Fe content. Since no significant crystalline Fe phases could be detected, with the possible exception of sheet silicates and very minor magnetite, together with the IR data it can be concluded that ferrihydrite is the major Fe

phase in these samples. Small amounts of orthoclase, montmorillonite, vermiculite, magnetite and dolomite were also detected.

SEM-EDS analyzes confirm the XRD results. However, SEM analyzes where performed on a slightly wider range of samples. The main minerals found are quartz, kaolinite and phyllosilicate minerals. Kaolinite and phyllosilicate minerals showed increased content of Fe. Electron microscopy studies reviled also minor mineralization, such as detrital grains of zircon, titanium oxides, monazite, and small grains of gold in all investigated samples. The iron oxyhydroxides was present in all samples. However, it seems that their amounts increase with the depth of the core. They generally form small aggregates with kaolinite and other phyllosilicates, the size of which is up to several hundred microns (Fig. 7). Fe oxyhydroxides in all samples have a similar EDS signal, except for samples from the depths of 9 and 50 cm of the core, whose chemical composition may corresponds to schwertmannite (Fig. 7D). Unfortunately, the rest of Fe oxyhydroxides present in the samples cannot be distinguished by EDS, but observing their morphology, it can be assumed that all samples may contain two different iron oxyhydroxides (Fig. 8).

3.2.5. Diatom analysis

A total of 60 diatom taxa belonging to 35 genera were identified. More than 300 valves could be identified in only four samples (1, 8, 9 and 10). In the remaining ones, the frequency of diatoms was not as high as required by statistical calculations. Samples with a low content of diatoms were similar to each other. Between 10 and 55 cm, the abundance of diatoms was very low and the number of valves does not exceeded 100 (statistically insignificant). Benthic, acidobiontic and acidophilous taxa prevailed in the assemblage. The most common species were *Eunotia nymanniana* Grunow, *E. exigua* (Brébisson ex Kützing) Rabenhorst, *Pinnularia appendiculata* (C. Agardh) Schaarschmidt and *Nitzschia palea* (Kützing) W. Smith. Diatoms teratogenically altered or covered with fine minerals have also been observed, making their identification difficult.

In three subsequent samples from the range of 8 - 10 cm, the number of diatoms increased significantly (over 300 valves). The species diversity varied from 45 to 50 taxa. Planktonic species appeared in relevant frequency with a simultaneous decline of benthic taxa. The expansion of planktonic diatoms mainly concerned alkaliphilous taxa, such as *Aulacoseira granulata* (Ehrenberg) Simonsen (over 18%), *A. pusilla* (Meister) Tuji and Houki (up to 10%) and *Cyclostephanos dubius* (Fricke) Round (above 5%). The increase of *Planothidium lanceolatum* (Brébisson ex Kützing) Lange-Bertalot (up to 8%), has also been recorded. Additionally, many previously unseen species have appeared, such as *Asterionella formosa*

Hassall, *Meridion circulare* (Greville) C.Agardh, *Navicula cryptocephala* Kützing or *Stephanocyclus meneghiniana* (Kützing) Kulikovskiy.

Between 1 and 8 cm, only single, damaged and often not identifiable diatoms were observed of *Pinnularia spp.*, *Eunotia spp*., *Nitzschia spp*. and *Fragilaria spp*. In the first, surface sample, the abundance of diatom frequency has been recorded again (above 300 valves), but with less species diversity (only 11 taxa). This sample contained the same dominant taxa as in ranges of 1 - 8 cm and 10 - 55 cm. The sudden disappearance of *Aulacoseira spp.*, *C. dubius* and other planktonic species, as well as *P. lanceolatum*, was detected. Again, acidophilous (*E. nymanniana* and *P. appendiculata*, 35% each) and acidobiontic (*E. exigua*, 16%) diatoms dominated the community.

3.2.6. DI-pH modeling

The reconstruction of the past water pH was based on diatoms from only four samples (1, 8, 9 and 10) where the frequency of valves was statistically significant (> 300). The root-mean square error for the training set (RMSE) was 0.49 and the coefficient of correlation (R2) was 0.94. The fluctuations of the water pH in ŁK-61 were as follows: 3.19 (1 cm), 7.02 (8 cm), 7.13 (9 cm), and 6.99 (10 cm). Changes in DI-pH values were large and amounted to 3.94 pH units. In the modern calibration data set, the occurrence of fossil diatoms has ranged from 89.6 to 100%. According to the modern analogue technique (MAT analysis), the minDC values were as follows 45.9 (1 cm), 133.2 (8 cm), 122.4 (9 cm) and 128.3 (10 cm). The threshold above which fossil taxa have no close analogues in the training set was 72.5. It appears that samples 8, 9 and 10 should be treated with caution.

4. Discussion

4.1. Surface and lake water

4.1.1. General characteristic

ŁK-61 Lake was classified into the group of the youngest pit lakes in the so-called ‘anthropogenic lake district’ in the Muskau Arch in western Poland characterized by the lowest values of water pH and the highest values of EC and hardness (Oszkinis-Golon et al., 2021; Pukacz et al., 2018). The relatively high content of total dissolved solids (TDS >1960 mg L^{-1}) reflected in the elevated EC values of lake water can be explained by the good solubility of solids in an acidic environment (e.g. España et al., 2008; Friese et al., 2013; Schultze et al., 2010; Stumm and Morgan 1981). Moreover, the negative correlation between the water pH and the sum of ions can be related to the degree and extent of mass input and pyrite dissolution in the study area (Friese et al., 2013). Similar features, such as low water pH and increased content of dissolved ions, such as Ca, Fe, Mg, Mn, and S, are characteristic of other pit lakes located in

close proximity to ŁK-61 Lake (Pukacz et al., 2018). The resemblance between these lakes can be explained by their similar age and origin, as they were formed as a result of the exploitation of the same lignite seam (Koźma, 2009; Pukacz et al., 2018; Sienkiewicz and Gasiorowski, 2016). One of the distinguishing features of ŁK-61 is the lower concentration of Fe and Al in the lake water compared to surroundings lakes, which is probably due to differences in the bedrock geology (Bartczak and Gancarz, 1998; Lutyńska and Labus, 2015).

An important source of dissolved solids in ŁK-61 is its tributary, which is indicated by the similar elemental composition of the surface layer of the lake water column and the lake's inflow (Table S1). The elemental composition of the water of ŁK-61 Lake is dominated by S and Ca, which was also observed in some pit lakes in the Lusatian lignite district in Germany (Friese et al., 1998). Other elements dominant in the lake water are Fe and Mg, but they are present in lower concentrations compared to Ca and S (Table S1). The increased content of Fe and S is likely a result of pyrite oxidation in the study area (Geller et al., 2013; Labus and Skoczyńska-Gajda, 2013). The elevated concentrations of Ca and Mg can therefore be related to the consequences of buffering of acidity caused by this process (dissolution of carbonates, silicates, etc.), weathering of mineral components of rocks forming embankments and mining area, as well as the elemental composition of water supplying this reservoir (e.g., Schultze et al., 2010; Wisotzky, 1998). In addition to the major elements, elevated concentrations of heavy metals (e.g., Co, Ni, Zn) were also noted, which is also likely the result of pyrite weathering in this area (Fig. 3; Table S1) (Wisotzky, 1998). Although it should be noted that the observed values are not as high as, for example, in some pit lakes of the Iberian Pyrite Belt in Spain (Sánchez España et al., 2008).

The available literature data showed that the physicochemical parameters and elemental composition of the water of ŁK-61 Lake have not changed significantly over the years, apart from episodic changes (Bożęcki, 2013; Gąsiorowski et al., 2021; Lutyńska and Labus, 2015; Oszkinis-Golon et al., 2021; Pukacz et al., 2020). This indicates that the process of neutralization of ŁK-61 Lake is very slow, which is considered typical for pit lakes with extremely acidic water (pH <3) (Sienkiewicz and Gasiorowski, 2016). To our knowledge, one of the significant changes in the physicochemical parameters and the elemental composition of the lake water was observed by Bożęcki (2013) in the summer of 2010 (Fig. 3; Table 1; S1). At that time, a significant increase in pH (up to 5.3) and a decrease in conductivity (EC = 268 µS cm^{-1}) of the lake water was noted, which was probably caused by the flood in early August 2010 (Bożęcki, 2013; MKOO, 2010). Moreover, a significant decrease in the content of Cl^-,

NO_2^-, SO_4^2, Ca, Fe, Mg, Mn, and Na, and an increase in the content of NO_3^-, PO_4^{3-} in the water of ŁK-61 Lake was also observed at that time.

4.1.2. Factors controlling the distribution of major elements and heavy metals in the water column

The conducted research showed that ŁK-61 is a stratified lake, which has also been described by Gąsiorowski et al. (2021). Development of stratification in water column was observed in other pit lakes in this area (e.g. Lutyńska and Labus, 2015), as well as in Germany (e.g. Schultze et al., 2010), the Czech Republic (e.g. Hrdinka et al., 2013), or Spain (e.g. Sánchez España et al., 2008). The stratification of ŁK-61 Lake is similar, for example, to Cueva de la Mora, Filón Centro (Tharsis), or Herrerías pit lakes in Spain, which are characterized by oxygenated mixolimnion and anaerobic monimolimnion, where an increase in water pH and the content of total dissolved solids was observed (Sánchez España et al., 2009). The vertical distribution of the content of selected elements in the water column of ŁK-61 Lake showed similar patterns, as in other stratified pit lakes, where the concentration of dissolved Fe increase in the bottom zone (Fig. 3; Table S1) (e.g., Friese et al., 2013; Ramstedt et al., 2003; Sánchez España et al., 2009). This phenomenon can be associated with the limited supply of oxygen to the hypolimnion, which causes that some substances (e.g., ferrous iron, sulfide, DOC) are in a chemically reduced form (Boehrer et al., 2017). Moreover, it can be also the result of the reductive dissolution of poorly crystalline Fe(III) secondary minerals, which leads to the release of Fe^{2+} and SO_4^{2-}, and an increase in the pH (>5) of the lake water (e.g., Sánchez España et al., 2009; Vithana et al., 2015). The development of reducing conditions responsible for these processes might also be related to oxygen consumption in the bottom zone of ŁK-61 due to the decomposition of OM, which can be transported to the studied lake from its catchment area (Boehrer and Schultze, 2008; Davison et al., 1993; Ramstedt et al., 2003; Stumm and Morgan, 1996).

Similarly to Fe, the content of K also increase in the hypolimnion of ŁK-61 Lake, which can be hypothetically related to the reductive dissolution of sulfate minerals (e.g. K-jarosite) under anoxic conditions (Dutrizac, 2008; Hrdinka et al., 2013). On the other hand, this hypothesis may be questionable in our case because the water pH in the epilimnion (pH = 2.85) is higher than that in which jarosite is commonly formed (pH <2.5) (Paikaray, 2020; Sánchez España et al., 2009). Moreover, the geochemical modeling indicated that the lake water of ŁK-61 is unsaturated with respect to the jarosite under prevailing conditions (SI =). Another reason for the increase in K concentrations downwards through the water column may be the decomposition of aluminosilicates (e.g., potassium feldspar), which can be components of the

rocks forming the embankments of ŁK-61 Lake and its catchment area (Bożęcki, 2013; Hrdinka et al., 2013; Lutyńska and Labus, 2015).

The vertical distribution of Mn concentrations in the water column of ŁK-61 Lake does not follow the same trend as in the case of Fe and S, although reductive dissolution of Mn secondary minerals has been observed in pit lakes (Davison et al., 1993; Friese et al., 1998; Sánchez España et al., 2009; Schultze et al., 2017). In addition, other elements (including heavy metals) associated with these minerals by co-precipitation/precipitation and sorption processes, were also expected to be released into the aqueous phase (Hrdinka et al., 2013; Sánchez España et al., 2009; Shi et al., 2021; Torres et al., 2013). Such an increase in the content of Fe and Mn downwards through the water column together with Ca, K, Na, and Mg was observed, for example, in the Udden pit lake in northern Sweden (Ramstedt et al., 2003). However, in our case, an opposite trend was observed in the vertical distribution of the content of particular major elements (e.g., Al, Ca, Mg, Mn, Si) and heavy metals (e.g., Co, Cu, Ni, Pb, Zn) in the collected water column (Fig. 3; Table S1). We assume that this phenomenon can be explained by the sorption of these elements by more thermodynamically stable Fe secondary minerals (as poorly crystalize goethite), which do not dissolve under prevailing conditions (Fig. 7, 8; Table S6, S7) (Shi et al., 2021). Some major and trace elements can also be captured by Al precipitates, such as kaolinite, which crystallization in the hypolimnion of ŁK-61 was indicated by the geochemical modelling and confirmed by the mineralogical analyses (Fig. 5, 6; Table S7) (Nordstrom and Ball, 1986; Sánchez-España et al., 2006; 2016; Schultze, 2013). A similar phenomenon was observed, for example, in Cueva de la Mora pit lake in Spain, where the precipitation of Al oxyhydroxysulphates (e.g. alunite) with the depth of the water column was related to simultaneous adsorption/co-precipitation of Cu (Sánchez España et al., 2009). We also suspect that the decrease in the content of some of heavy metals in the hypolimnion of ŁK-61 (pH >6) might be explained by their retention by allochthonous Al-bearing minerals, e.g. clay minerals, which shows much better sorption properties with increasing pH (Jiang et al., 2010).

It can also be assumed that the precipitation of metal sulfides may led to a decrease in the trace metals content across an oxic-anoxic interface, as for example, in the Sancho Reservoir in Spain (Friese et al., 1998; Ramstedt et al., 2003; Schultze et al., 2017; Torres et al., 2013). However, this hypothesis may be questionable in our case, because the mineralogical analysis did not reveal the presence of metal sulphides (except for framboidal pyrite) in the examined samples of lake sediments. Vink et al. (2010) suggested that DOC may provide bonding sites for trace elements released by the reductive dissolution of Mn and Fe (oxy)hydroxides, when

sulfides have not yet been formed (Davis 1984; Christensen et al. 1999; Eyrolle et al., Benaim, 1999). This may theoretically apply to our case, as the content of DOC in the bottom zone of ŁK-61 increase significantly to 32.7 mg L^{-1}, however, additional analyses would be needed to better support the hypothesis (Fig. 3).

4.2. Lake sediments

4.2.1. Factors controlling distribution of major elements and heavy metals in lake sediments

The presented studies showed that ŁK-61 is an acidic pit lake (pH <3) with sediments close to neutral, which can be deducted from the pH of the lake water (pH >6) measured in the bottom zone (pore water pH was not measured) of the studied lake (Fig. 3; Table 1). Friese et al. (1998) suggested that the production of alkalinity in these types of lakes is related to the reduction of sulfates and degradation of OM. Compared to a lake of this type, such as ML-Halbendorf in the Lusatian lignite district in Germany, ŁK-61 Lake is characterized by bottom sediments with a relatively similar content of Fe and particular trace metals, such as Cu, Ni, and Zn (Table S2) (Friese et al., 1998). The difference can be seen mainly in the concentrations of Al and Mn, which in our case were much higher than in the lake sediments of ML-Halbendorf. Moreover, the Fe content in the surface layer of the collected sediment column (213 g kg^{-1}) was relatively similar to that found in Waldsee Lake (269 g kg^{-1}) in the Lusatia, where also in the hypolimnion the water pH is about 6 and anaerobic conditions prevail (Friese, 2004). Compared to the elemental composition of the bottom sediments of other pit lakes in the Muskau Arch in Poland, the surface lake sediments of ŁK-61 contain higher amounts of Al and Fe, and lower amounts of Ca, Mn and P (Gąsiorowski et al., 2021). On the other hand, pit lakes located in the close proximity to ŁK-61 Lake (sites 57-62; according to Gąsiorowski et al. (2021)) are characterized by bottom sediments with a slightly higher content of Fe, and in some cases also Mn, which likely indicate differences in the bedrock geology (Bartczak and Gancarz, 1998).

The elevated content of Fe in the sediments of ŁK-61 Lake is related to high abundance of Fe(III) secondary minerals, such as ferrihydrite, which is considered one of the most common minerals in soils and sediments (Fig. 6) (Shi et al., 2021). Other Fe precipitates, such as schwertmannite, were found in samples collected from deeper layers of the sediment column (e.g., at 9 and 50 cm depth) (Fig. 7 C, D). We suppose that its precipitation could have been related to the changes in physicochemical conditions in ŁK-61 Lake over time, which was discussed in more detail in Section 4.2.3. It can be also assumed that some amounts of goethite could also have been formed as a result of transformations of thermodynamically unstable

mineral phases, such as schwertmannite and ferrihydrite (Bigham et al., 1996; Burton et al., 2008; Cudennec and Lecerf, 2006; Paikaray, 2020; Vithana et al., 2015).

The content of Al in the surface layer of the collected core (67.7g kg^{-1}) was only slightly lower than that measured, for example, in the surface lake sediments (99.3 g kg^{-1}) of ŁK-41 Lake (water pH = 7.4), which was formed as a result of clay mining in the Muskau Arch in Poland (Gąsiorowski et al., 2021; Sienkiewicz and Gąsiorowski, 2018). This phenomenon may be related to the presence of large amounts of phyllosilicates (e.g. kaolinite) in the lake sediments of ŁK-61, which are probably transported from located nearby deposits of kaolinite clays (Fig. 5, 6) (Koźma 2009; Gruszecki et al., 2006). The presence of Al-bearing minerals in the bottom sediments of ŁK-61 can also be related to the physical disaggregation of pit walls and embankments (Sánchez España et al., 2008). We also suspect that some of Al precipitates crystallize directly from the water column of ŁK-61 Lake, as indicated by geochemical modelling (Table S7) (see Section 4.1.2.). However, the distinction between authigenic and allogenic kaolinite in the examined samples was difficult, as also noted by Sánchez-España et al. (2016). Titanium, another dominant element (arithmetic mean = 6.5 g kg^{-1}) in the bottom sediments of ŁK-61, seems to be associated with Al (R_s = 0.86) (Table S5). This relationship can be explained by fact that kaolinite clays occurring in this region are relatively rich in TiO_2 (about 1.7 wt.%) (Gruszecki et al., 2006). Probably for this reason, numerous Ti oxides were found in selected samples of lake sediments during SEM-EDS analyses.

Potassium was the next most abundant element in the collected lake sediments of ŁK-61 Lake (arithmetic mean = 14.5 g kg^{-1}). This phenomenon is likely related to the presence of K-bearing minerals, such as feldspars and clay minerals, which were found in the examined lake sediments during SEM-EDS analyses. We suppose that these minerals are likely supplied to the studied lake from its catchment area. This hypothesis might be supported by a significant positive correlation between the content of K and ^{40}K (R_s = 0.94), which can be an useful indicator of the presence of allochthonous K-bearing minerals (Bobos et al., 2021; Madruga et al., 2014; Somboon et al., 2018). The crystallization of K precipitates (e.g. K-jarosite) is rather doubtful in our case, as has already been discussed (see Section 4.1.2.). Some amounts of K, as well as other major elements, such as Ca, Na, Mg, Ba, Sr, and P, was also found to be adsorbed on the surface of clay minerals and Fe (oxy)hydroxides (Fig. 7). Moreover, only a few minerals containing other major elements, such as Ca (e.g., gypsum) and Ba (e.g., barite) were found in the examined lake sediments during SEM-EDS analyses. This phenomenon may be explained by the fact that the presence of some major elements, such as Ca, in the form of authigenic chemical precipitates is rather unlikely at a water pH <3 (Sánchez España et al., 2008).

Heavy metals (such as Cr, Ni, Pb, Zn) are likely associated in the bottom sediments of ŁK-61 Lake with Fe (oxy)hydroxides, through co-precipitation from the water column (Cánovas et al., 2007; Hierro et al., 2014; Shi et al., 2021). Moreover, some of these elements can be absorbed/adsorbed onto Fe precipitates, which are characterized by good retention capacity due to their large surface areas and high reactivity (Acero et al., 2006; Makvandi et al., 2021; Rose and Bianchi-Mosquera, 1993; Zhu et al., 2012). Similarly, some of these trace metals could have co-precipitated with Al secondary minerals (e.g. kaolinite) (see Section 4.1.2.). Moreover, studied heavy metals could have also been captured by allochthonous Al-bearing minerals (e.g. clay minerals) supplied to ŁK-61 Lake because of their good retention capacity (e.g., Carrero et al., 2015; Durrant et al., 2018; Jiang et al., 2010).

4.2.2. Factors controlling distribution of radionuclides in lake sediments

^{210}Pb and its decay product ^{210}Po are probably immobilized in the bottom sediments of ŁK-61 Lake by Fe and Al precipitates, as well as by allochthonous solid particles (e.g., clay minerals) supplied to the studied lake (Carvalho et al., 2017; Cook et al., 2018; Ram et al., 2021; Shi et al., 2021). ^{210}Po can also be also associated with Mn-bearing minerals, as indicated by a moderate positive correlation between the content of ^{210}Po and Mn (R_s = 0.53) in the bottom sediments of ŁK-61 (Table S5) (Benoit and Hemond, 1990; Carvalho et al., 2017). The presence of these radioisotopes may be also related to sulfates (e.g. anglesite, barite, celestine, gypsum), which can be good hosts for ^{226}Ra, and indirectly also for its daughter radioisotopes, including ^{210}Pb and ^{210}Po (Cook et al., 2018). On the other hand, this hypothesis may be doubtful, since only a few barite and gypsum crystals were found in the examined samples of lake sediments during SEM-EDS analyses. Moreover, it is rather unlikely that these radionuclides were captured by sulfides, since the presence of these minerals in the collected lake sediments was rather rare (Carvalho et al., 2017; Ram et al., 2019).

Calculating the age of the collected sediments from ŁK-61 Lake was impossible using the ^{210}Pb dating method. This is because the down-core profile of ^{210}Po activity concentrations (assuming equilibrium with ^{210}Pb) was significantly disturbed and did not follow the exponential curve, as can be theoretically expected in undisturbed sediment profiles, according to the law of radioactive decay (Appleby, 2005; Swarzenski, 2014). Similar disturbances in the vertical distribution of ^{210}Po activity concentrations were observed in the sediment columns collected from lakes affected by increased sulfur and nitrate input – Mały Staw (pH = 6.2) and Wielki Staw (pH = 5.2) in Sudety Mountains in Poland (Sienkiewicz et al., 2006). In these lakes, however, as a possible cause of such disturbances was given landslips from the catchment area, sediment slumps, and avalanches. Similar disturbances, as in our case, observed in the

down-core profile of ^{210}Pb activity concentrations of TR-33 Lake (pH = 6.5) in the Muskau Arch in Poland was associated with horizons of clay interbeddings (Sienkiewicz and Gasiorowski, 2016). We suspect that this phenomenon in ŁK-61 may be rather related to another than above-mentioned depositional events (e.g., flood), which is disused in more details in Section 4.2.3.

^{137}Cs deposited in the bottom sediments of ŁK-61 Lake is probably originated from its direct atmospheric deposition after the Chernobyl accident, as well as from the subsequent wash off solids and OM (which could have integrated ^{137}Cs during its initial deposition) from the surrounding soils (e.g., Ashraf et al., 2014; Beresford et al., 2016; Naulier et al., 2017). The concentrations of ^{137}Cs activity in the surface lake sediments (1.0 ± 0.3 Bq kg^{-1}) of ŁK-61 are much lower compared to, for example, the Turawa Dam Lake (southwestern Poland), where the highest content of ^{137}Cs in the surface lake sediments was 103 ± 12 Bq kg^{-1} (Sekudewicz and Gąsiorowski, 2022). This difference is most likely related to the fact that the average value of ^{137}Cs deposition in the soils (0.39 ± 0.10 kBq m^{2}) of the Lubuskie Voivodship (where ŁK-61 Lake is located) is one of the lowest compared to other provinces of Poland (Isajenko et al., 2022). For comparison, the maximum concentration of ^{137}Cs activity (9.4 ± 2.0 Bq kg^{-1}) measured in the collected sediment profile was slightly lower to those found in other pit lakes in the Muskau Arch in Poland, e.g., in 17 (16.2 ± 3.4 Bq kg^{-1}; water pH = 5.2) or 46 Lakes (20.9 ± 3.6 Bq kg^{-1}; water pH = 3.6) (unpublished data; sites according to Gąsiorowski et al., 2021).

^{137}Cs was probably mostly immobilized in sediments of ŁK-61 Lake as a result of its sorption by clay minerals (Park et al., 2021; D.E. Walling and Quine, 1993; Zapata and Nguyen, 2009). This is because Cs^{+} has a strong affinity to the 2:1 layer clays (e.g., illite, smectite group) (Cornell, 1993; Durrant et al., 2018; Mukai et al., 2016; Park et al., 2019; Sawhney, 1972). Moreover, ^{137}Cs can be associated with 1:1 layered clays, such as kaolinite, which is quite common in the bottom sediments of ŁK-61 (Fig. 5). On the other hand, sorption onto kaolinite can be much less efficient than onto 2:1 layered clays, due to its lower cation exchange capacity (CEC) and absence of frayed edge sites (FES) (Durrant et al., 2018). Moreover, the uptake of ^{137}Cs by clay minerals may be limited in ŁK-61, as the competition between Cs^{+} and H^{+} ions may occur at low pH (<4) (Belousov et al., 2019; Fuller et al., 2014). On the other hand, Fuller et al. (2014) suggested that this may be significant in the case of high concentrations of ^{137}Cs (allowing for FES saturation). It can be also assumed that the precipitation of Fe(III) (oxy)hydroxides or other compounds in ŁK-61 has a rather dubious effect on ^{137}Cs retention, since its co-precipitation is rather negligible (Lieser and Steinkopff, 1989). Similarly, ^{137}Cs adsorption onto Fe or Al precipitates is rather unlikely, as it was found that the presence of

monovalent cations (e.g., $K^{+,}$ Na^{+}) can practically eliminate Cs^{+} adsorption (McKinley et al., 2001).

Based on the data obtained, it was difficult to determine whether the peak of ^{137}Cs activity concentrations observed at the depths of 7 - 11 cm of the collected sediment column corresponds to the Chernobyl fallout, or rather the elevated content of this radioisotope in the deeper parts of the core (>50 cm depth) is related to this event. This is due to the fact that the elevated concentrations of ^{137}Cs activity in this part of the core coincides with the disturbances in the vertical distribution of concentrations of other studied elements (e.g., Cu, Ni, Pb, Mg, Sr) (Fig. 4; Table S2, S5). Their common origin may confirm the positive correlation between the content of radiocesium and some heavy metals, such as Ni (Rs = 0.80) and Pb (Rs = 0.74) (Table S5). For this reason, it was not possible to calculate the age of the collected lake sediments using the ^{137}Cs dating method. We suspect that the increased content of ^{137}Cs in this sediment layer may be the result of a flood event (see section 4.2.3).

4.2.3. The potential impact of a flood on the distribution of selected heavy metals and radionuclides in lake sediments

As already mentioned, the vertical distribution of HMR content was significantly disturbed in the upper part of the sediment profile collected from ŁK-61 Lake (Fig. 4). The observed disturbances can be related to the post-depositional processes taking place in the sediment column, changes in sedimentological conditions in the studied lake over time, as well as episodic depositional events (e.g. floods). We suspect, for example, that an increase in the concentration of e.g., Ca, Mn, Fe, and S in the top part of the collected core (0-3 cm depth) can be related to the presence of (oxy)hydroxides and carbonates that have not yet been dissolved under reducing conditions (see Section 4.1.2.). On the other hand, an almost threefold increase (compared to the average) in the content of some major (e.g. Na, P) and trace metals (e.g., Cu, Zn), and radionuclides (^{137}Cs and ^{210}Po) between 7 and 12 cm of the depth of the collected sediment column cannot be explained in this way (Fig. 4). Such an increase in, for instance, the content of Ni and Zn in the top sediment layer in ML-F Lake in the Lusatian lignite district in Germany was explained by the change from aerobic to anaerobic conditions and the precipitation of metal sulfides (Friese et al., 1998). In our case, however, such explanation may be questionable because the presence of metal sulfides (except framboidal pyrite) in the examined lake sediments cannot be confirmed (see Section 4.1.2.). In addition, the distribution of HMR in the bottom sediments of ŁK-61 do not seem to be related to the cycling of Fe and S, as there is no significant correlation between their content (Table S5).

The most likely scenario explaining such behavior of the studied elements may be a change in the physicochemical parameters of lake water of ŁK-61 in the past, which can be indicated by the diatom-inferred pH model performed for lake sediments collected from the depths of 8 - 10 cm of the core (pH ~7±0.5). We suppose that this change was related to the flood in the summer of 2010, which led to an increase in the pH of the lake water from 2.9 to 5.3 (Fig. 3; Table 1) (Bożęcki; 2013). At that time, a decrease in the content of, e.g., Fe, Mn, Ca, Na, SO_4^{2-}, Cl^-, and an increase in the content of NO_3^- and PO_4^{3-} in the lake water of LK-61 was also observed (Table S1). Such a decrease in the concentration of the above-mentioned elements in lake water of ŁK-61 could have been related at that time to the 'dilution effect', as well as to the co-precipitation/precipitation and/or adsorption of particular elements onto newly formed mineral phases (e.g., schwertmannite), which crystallization in ŁK-61 is rather unlikely under current conditions (Table S7). The presented hypothesis may be supported by geochemical modeling performed on the basis of data presented by Bożecki (2013), as well as mineralogical analyses of selected lake sediments (Fig. 7 C; Table S8). Similar phenomenon was observed, for example, in the Rio Tinto River in Spain, where water oversaturated in kaolinite was found only when pH increased (>5) during high floods (Cánovas et al., 2007). We suspect that, in our case, as a result of this process, certain amounts of heavy metals and radionuclides were retained and buried in the bottom sediments of ŁK-61, giving a characteristic peak of their content in the sediment record (Fig. 4).

The increase in HMR content in this part of the sediment column of ŁK-61 can be also explained by the input of particles carried by the flood, which (as fresh sorption sites) could have captured pollutants, as observed e.g., in the Coledale Beck catchment in the UK (Mayes et al., 2021). Moreover, the influx of buffering sedimentary material (e.g. calcite) could have caused the lower acidity of lake water at that time (Fig. 3; Table 1) (Bożęcki, 2013; Herzsprung et al., 2010). An increase in water pH could, in turn, additionally enhance the sorption of pollutants onto detrital material supplied to ŁK-61, such as kaolinite, which shows better sorption properties at higher pH (Jiang et al., 2010). Flood could also transported to the studied lake contaminated particles with heavy metals, radionuclides or phosphorus, as was observed, for example, in Goitsche Lake in Germany (Herzsprung et al., 2010). Confirmation of this hypothesis, in our case, can be for example, the increased content of ^{137}Cs, which is known as an important indicator of soil erosion and its redistribution, at the depths of 7 - 12 cm of the collected core (Fig. 4) (Walling and Quine, 1993; Zapata and Nguyen, 2009). In addition, a significant positive correlation between the content of ^{137}Cs and some heavy metals (e.g., Ni, Pb) in the bottom sediments of ŁK-61 may additionally indicate their probable common origin

(Table S5). It is also possible that the source of pollution was also the Nysa Łużycka River, which could have transported ^{210}Po (and presumably also ^{210}Pb), as it was found that the annual surface flow for ^{210}Po is relatively high (245 kBq year^{-1}) in this river (Skwarzec et al., 2012). It can be also assumed that the Nysa Łużycka River were also transported some amounts of other elements, such as Mn, P, N, Sr, and Zn, as evidenced by a moderate positive correlation between their content and ^{210}Po activity concentrations in the collected lake sediments (Table S5).

Additional evidence that the flood could have affected the distribution of heavy metals and radionuclides in the bottom sediments of ŁK-61 might be the presence of allochthonous OM (e.g. vascular land plants) in the samples collected from the depths of 7 - 10 cm of the collected core, as indicated by an increase in the C/N ratio (>20) (Meyers and Ishiwatari, 1995). The presented hypothesis may also be supported by an increase in the TN content in this part of the sediment column, which theoretically may correspond to the increase in the concentration of NO_3^- in the lake water of ŁK-61 in August 2010 (Fig. 4; Table S1) (Bożęcki, 2013). It can be also suspected that studied radionuclides were also supplied with allochthonous OM, as it is known that they can be associated with biological particles (microplankton, bacteria, etc.) (Carvalho et al., 2017; Stewart et al., 2007). In cannot be ruled out that a particle organic matter (e.g., diatoms, which were more abundant at the depths of 8-10 cm of the core), could also have provided new sorption sites for pollutants and thus affect their retention and accumulation in the bottom sediments of ŁK-61 (Kleeberg and Grüneberg, 2005; Paulsson and Widerlund, 2021; Schultze, 2013). On the other hand, we assume that sorption of ^{137}Cs was rather related to the presence of e.g., clay minerals rather than diatoms, because diatomite was found to have a rather low sorption capacity of Cs^+ (Belousov et al., 2019).

The alternative hypotheses explaining such a behavior of selected heavy metals and radionuclides in the upper part of the sediment column of ŁK-61 may be fertilizers that could have been delivered from the surrounding areas e.g., along with the flood. The increased content of ^{210}Po and P may theoretically confirm this hypothesis, because phosphate fertilizers are known to be the main anthropogenic source of ^{210}Pb and ^{210}Po (Barbero et al., 2014; Carvalho et al., 2017). Paulsson et al. (2023) also pointed out that remediation of pit lakes (e.g. by liming) can also raise the pH of the lake water, and thus cause the precipitation of secondary minerals along with contaminates. However, due to the lack of data, we assume that it is more likely that the source of nutrients (such as N and P) deposited in the bottom sediments of ŁK-61 were fertilizers, which were probably transported to the lake with the flood from the surroundings areas (Fig. 4). This can be hypothetically confirmed by an increase in the concentration of NO_3^- and PO_4^{3-} observed by Bożęcki (2013) in the lake water of ŁK-61 in the summer of 2010 (Table

S1). Moreover, the increased content of ^{137}Cs at the same depth of the collected core as the mentioned elements may theoretically confirm this assumption, as this radionuclide is rather not intended to be present in the remediation components.

5. Conclusions

The main processes responsible for the distribution of selected heavy metals and radionuclides in the acidic pit lake ŁK-61 in the Muskau Arch in Poland are 1) mineral dissolution, 2) crystallization of Fe and Al precipitates and/or 3) sorption by allogenic and autochthonous particles. Geochemical modelling showed that Fe-bearing minerals (e.g., goethite, hematite) are most likely to precipitate in the epilimnion (pH <3) of ŁK-61, while in the hypolimnion (pH >5), where reducing conditions prevail and DOC content increases, Al-bearing minerals (e.g., alunite, kaolinite) may also be formed. We assume that this phenomenon is responsible for the retention of some major elements (e.g., Al, Ca, Mg, Mn, Si) and trace metals (e.g., Co, Ni, Pb, Zn), which concentrations decrease significantly in the hypolimnion of ŁK-61. The increase in the content of other elements, such as Fe and S, in this part of the lake's water column probably result from the microbial reductive dissolution of poorly crystalline Fe (oxy)hydroxides. On this basis, we suspect that that DOM and possibly also bacteria affect the geochemical behavior of these elements in the lake water of ŁK-61, but further research should be conducted to support this hypothesis.

The geochemical behavior of the studied elements in ŁK-61 may also be significantly affected by its tributary, which can be an important source of dissolved solids, as evidenced by the similar elemental composition of surface lake water and lake's inflow. Moreover, the supplied detrital material from the catchment area may also importantly influence the distribution of heavy metals and radionuclides in the lake sediments of ŁK-61, as they may constitute fresh sorption sites for dissolved solids and/or be a source of polluted particles. The influx of detrital material can be confirmed by analysis of the mineralogical composition of the bottom sediments of the studied lake, which showed the presence of allogenic minerals (e.g. quartz, clay minerals). Additionally, it may also be confirmed by the presence of relatively numerous accessory minerals (e.g. Ti oxides, zircons, monazites) in the collected samples of lake sediments.

The obtained results also showed that the sedimentation conditions in ŁK-61 was significantly disturbed in the past, which can be deducted from the vertical distribution of the content of selected elements and radionuclides in the upper part of the collected sediment profile. For this reason, it was impossible to calculate the age of the collected lake sediments with the ^{137}Cs and ^{210}Pb dating methods. The observed disturbances were particularly visible

between 7 and 12 cm depth of the collected core, where the content of selected major elements (e.g. Ca, Mg, Mn, P, TN), trace elements (e.g. Cu, Ni, Pb, Zn), and radioisotopes (^{137}Cs and ^{210}Po) was elevated. We assume that this phenomenon may be related to the flood in August 2010, which caused an increase in the water pH of ŁK-61 from 3 to over 5 (according to literature data). This hypothesis can be confirmed by reconstructed diatom-inferred pH changes. We suspect that as a result of the increase in the pH of the lake water, fresh secondary solids (e.g. schwertmannite) may have crystallized and captured dissolved solids, as indicated by geochemical modeling and mineralogical analyses. It cannot be also ruled out that particles contaminated with heavy metals and radionuclides were delivered to ŁK-61 from the surrounding areas by surface runoff and by the Nysa Łużycka River. Moreover, it is possible that the source of contamination were also fertilizers, which could have been delivered to ŁK-61 from the surrounding areas as a result of the flood, as can be indicated by increased concentrations of P and TN in the upper part of the collected core.

The conducted research allowed us for a better understanding of the processes responsible for the distribution of selected heavy metals and radioisotopes in an acidic pit lake, which can be in danger of flooding, and thus exposed to significant changes in the physicochemical parameters of the lake water. The obtained results may be particularly important in terms of treatment strategies for AMD-affected pit lakes, as well as in predicting the geochemical behavior of pollutants in similar lakes located in areas at risk of flooding. These results can be valuable in the case of the environmental protection, as heavy metals are toxic environmental pollutants that can pose a serious threat to living organisms. Moreover, they can also be important from the point of view of radioactive environmental monitoring in areas affected by AMD. It should also be emphasized that the conducted research showed that ^{137}Cs and ^{210}Po can be used as radiogeochronological fingerprints of depositional events (such as floods) recorded in the bottom sediments of pit lakes.

Acknowledgements

The authors would like to thank Elwira Sienkiewicz and Jacek Stienss from the ING PAS for their help during field work. We are thankful to Anna Mulczyk and Karolina Kaucha from the ING PAS for their help in laboratory work.

AWI, GFZ, IG PAS ?

Credit author statement

I. Sekudewicz: Conceptualization, Sample collection, Investigation, Formal analysis, Visualization, Writing – original draft. M. Syczewski: Formal analysis, Investigation. Jan Rohovec: Investigation. Š. Matoušková: Investigation. Urszula Kowalewska: Formal analysis, Investigation. Roberts Blukis: Formal analysis, Investigation. Ingrid Stimac: Investigation. M. Gąsiorowski: Sample collection, Supervision.

Funding

The project was supported by the internal project 'CEZ137' of the Institute of Geological Sciences of the Polish Academy of Sciences. This work was also supported by the Bekker Programme of the Polish National Agency for Academic Exchange (BPN/BEK/2021/1/00411).

Declaration of competing interest

The authors declare no competing interests.

Appendix A. Supplementary data

References

Abril, J.M., San Miguel, E.G., Ruiz-Canovas, C., Casas-Ruiz, M., Bolívar, J.P., 2018. From floodplain to aquatic sediments: Radiogeochronological fingerprints in a sediment core from the mining impacted Sancho Reservoir (SW Spain). Sci. Total Environ. 631–632, 866–878. https://doi.org/10.1016/j.scitotenv.2018.03.114

Appleby, P.G., 2002. Chronostratigraphic Techniques in Recent Sediments. Track. Environ. Chang. Using Lake Sediments 171–203. https://doi.org/10.1007/0-306-47669-X_9

Appleby, P.G., 2005. Chronostratigraphic Techniques in Recent Sediments, in: Tracking Environmental Change Using Lake Sediments. Kluwer Academic Publishers, pp. 171–203. https://doi.org/10.1007/0-306-47669-x_9

Appleby, P.G., 2008. Three decades of dating recent sediments by fallout radionuclides: A review. Holocene. https://doi.org/10.1177/0959683607085598

Ashraf, M.A., Akib, S., Maah, M.J., Yusoff, I., Balkhair, K.S., 2014. Cesium-137: Radio-chemistry, fate, and transport, remediation, and future concerns. Crit. Rev. Environ. Sci. Technol. 44, 1740–1793. https://doi.org/10.1080/10643389.2013.790753

Barbero, L., Gázquez, M.J., Bolívar, J.P., Casas-Ruiz, M., Hierro, A., Baskaran, M., Ketterer, M.E., 2014. Mobility of Po and U-isotopes under acid mine drainage conditions: an

experimental approach with samples from Río Tinto area (SW Spain). J. Environ. Radioact. 138, 384–389. https://doi.org/10.1016/j.jenvrad.2013.11.004

Bartczak E., Gancarz A., 1998. Szczegółowa Mapa Geologiczna Polski 1:50 000, sheet 645 – Łęknica (M-33-18-A), 646 – Trzebiel (M-33-18-B). Polish Geological Institute (PIG). https://bazadata.pgi.gov.pl

Belousov, P., Semenkova, A., Egorova, T., Romanchuk, A., Zakusin, S., Dorzhieva, O., Tyupina, E., Izosimova, Y., Tolpeshta, I., Chernov, M., Krupskaya, V., 2019a. Cesium sorption and desorption on glauconite, bentonite, zeolite, and diatomite. Minerals 9, 1–16. https://doi.org/10.3390/min9100625

Benoit, G., Hemond, H.F., 1990. 210Po and 210Pb Remobilization from Lake Sediments in Relation to Iron and Manganese Cycling. Environ. Sci. Technol. 24, 1224–1234. https://doi.org/10.1021/es00078a010

Beresford, N.A., Fesenko, S., Konoplev, A., Skuterud, L., Smith, J.T., Voigt, G., 2016. Thirty years after the Chernobyl accident: What lessons have we learnt? J. Environ. Radioact. 157, 77–89. https://doi.org/10.1016/j.jenvrad.2016.02.003

Bethke, C.M., 1996. Geochemical Reaction Modeling. Oxford University Press (397 pp.)

Bigham, J.M., Schwertmann, U., Traina, S.J., Winland, R.L., Wolf, M., 1996. Schwertmannite and the chemical modeling of iron in acid sulfate waters. Geochim. Cosmochim. Acta 60, 2111–2121. https://doi.org/10.1016/0016-7037(96)00091-9

Blasco, M., Gázquez, M.J., Pérez-Moreno, S.M., Grande, J.A., Valente, T., Santisteban, M., de la Torre, M.L., Bolívar, J.P., 2016. Polonium behaviour in reservoirs potentially affected by acid mine drainage (AMD) in the Iberian Pyrite Belt (SW of Spain). J. Environ. Radioact. 152, 60–69. https://doi.org/10.1016/j.jenvrad.2015.11.008

Bobos, I., Madruga, M.J., Reis, M., Esteves, J., Guimarães, V., 2021. Clay mineralogy insights and assessment of the natural (228Ra, 226Ra, 210Pb, 40K) and anthropogenic (137Cs) radionuclides dispersion in the estuarine and lagoon systems along the Atlantic coast of Portugal. CATENA 206, 105532. https://doi.org/10.1016/J.CATENA.2021.105532

Boehrer, B., Schultze, M., 2008. Stratification of lakes. Rev. Geophys. 46, RG2005. https://doi.org/10.1029/2006RG000210

Boehrer, B., von Rohden, C., Schultze, M., 2017. Physical Features of Meromictic Lakes: Stratification and Circulation 15–34. https://doi.org/10.1007/978-3-319-49143-1_2

Borch, T., Masue, Y., Kukkadapu, R.K., Fendorf, S., 2007. Phosphate imposed limitations on biological reduction and alteration of ferrihydrite. Environ. Sci. Technol. 41, 166–172. https://doi.org/10.1021/ES060695P/SUPPL_FILE/ES060695PSI20060930_030836.PDF

Bożęcki, P., 2013. Studium osadów tworzących się w obszarze eksploatacji węgla brunatnego w rejonie Łęknicy (Łuk Mużakowa) (in Polish). Kraków: Akademia Górniczo- Hutnicza im. Stanisława Staszica.

Burton, E.D., Bush, R.T., Sullivan, L.A., Mitchell, D.R.G., 2008. Schwertmannite transformation to goethite via the Fe(II) pathway: Reaction rates and implications for iron–sulfide formation. Geochim. Cosmochim. Acta 72, 4551–4564. https://doi.org/10.1016/J.GCA.2008.06.019

Cánovas, C.R., Olías, M., Nieto, J.M., Sarmiento, A.M., Cerón, J.C., 2007. Hydrogeochemical characteristics of the Tinto and Odiel Rivers (SW Spain). Factors controlling metal contents. Sci. Total Environ. 373, 363–382. https://doi.org/10.1016/J.SCITOTENV.2006.11.022

Cánovas, C.R., Peiffer, S., Macías, F., Olías, M., Nieto, J.M., 2015. Geochemical processes in a highly acidic pit lake of the Iberian Pyrite Belt (SW Spain). Chem. Geol. 395, 144–153. https://doi.org/10.1016/J.CHEMGEO.2014.12.007

Carlson, L., Schwertmann, U., 1981. Natural ferrihydrites in surface deposits from Finland and their association with silica. Geochim. Cosmochim. Acta 45, 421–429. https://doi.org/10.1016/0016-7037(81)90250-7

Carvalho, F., Fernandes, S., Fesenko, S., Holm, E., Howard, B., Martin, P., Phaneuf, M., Porcelli, D., Prohl, G., Twining, J., 2017. The environmental behaviour of polonium.

Cook, N.J., Ehrig, K.J., Rollog, M., Ciobanu, C.L., Lane, D.J., Schmandt, D.S., Owen, N.D., Hamilton, T., Grano, S.R., 2018. 210pb and210po in geological and related anthropogenic materials: Implications for their mineralogical distribution in base metal ores. Minerals 8. https://doi.org/10.3390/min8050211

Cornell, R.M., 1993. Adsorption of cesium on minerals: A review. J. Radioanal. Nucl. Chem. Artic. https://doi.org/10.1007/BF02219872

Cudennec, Y., Lecerf, A., 2006. The transformation of ferrihydrite into goethite or hematite, revisited. J. Solid State Chem. 179, 716–722. https://doi.org/10.1016/J.JSSC.2005.11.030

Christensen JB, Botma JJ, Christensen TH (1999) Complexation of Cu and Pb by DOM in polluted groundwater: a comparison of experimental data and predictions by computer speciation models (WHAM and MINTEQA2). Wat Res 15:3231–3238.

Davis, J. A. 1984. Complexation of trace metals by adsorbed nat-ural organic matter. Geochim. Cosmochim. Acta48:679–691.

Davison, W., Davison, William, 1993. Iron and manganese in lakes. ESRv 34, 119–163. https://doi.org/10.1016/0012-8252(93)90029-7

Durrant, C.B., Begg, J.D., Kersting, A.B., Zavarin, M., 2018. Cesium sorption reversibility and kinetics on illite, montmorillonite, and kaolinite. Sci. Total Environ. 610–611, 511–520. https://doi.org/10.1016/j.scitotenv.2017.08.122

Dutrizac, J.E., 2008. Factors affecting the precipitation of potassium jarosite in sulfate and chloride media. Metall. Mater. Trans. B Process Metall. Mater. Process. Sci. 39, 771–783. https://doi.org/10.1007/S11663-008-9198-7/FIGURES/22

Eyrolle F, Benaim JY (1999) Metal available sites on colloidal organic compounds in surface waters. Wat Res 4:995–1004

Flynn, W.W., 1968. The determination of low levels of polonium-210 in environmental materials. Anal. Chim. Acta 43, 221–227. https://doi.org/10.1016/S0003-2670(00)89210-7

Frank, M., Harrell, E., 2023. Package "Hmisc" Title Harrell Miscellaneous.

Friese, K., 2004. Depth distribution of heavy metals in lake sediments from lignite mine pit lakes of Lusatia (Germany). Stud. Quat. 21, 197–205.

Friese, K., Hupfer, M., Schultze, M., 1998. Chemical Characteristics of Water and Sediment in Acid Mining Lakes of the Lusatian Lignite District, in: Acidic Mining Lakes. Springer Berlin Heidelberg, pp. 25–45. https://doi.org/10.1007/978-3-642-71954-7_3

Fuller, A.J., Shaw, S., Peacock, C.L., Trivedi, D., Small, J.S., Abrahamsen, L.G., Burke, I.T., 2014. Ionic strength and pH dependent multi-site sorption of Cs onto a micaceous aquifer sediment. Appl. Geochemistry 40, 32–42. https://doi.org/10.1016/j.apgeochem.2013.10.017

Gąsiorowski, M., Stienss, J., Sienkiewicz, E., Sekudewicz, I., 2021. Geochemical Variability of Surface Sediment in Post-Mining Lakes Located in the Muskau Arch (Poland) and Its Relation to Water Chemistry. Water. Air. Soil Pollut. 232, 1–12. https://doi.org/10.1007/s11270-021-05057-8

Geller, W., Schultze, M., Kleinmann, R., Wolkersdorfer, C., 2013. Acidic pit lakes: The legacy of coal and metal surface mines. Environ. Sci. Eng. (Subseries Environ. Sci. https://doi.org/10.1007/978-3-642-29384-9/COVER

Hamilton NE, Ferry M (2018) ggtern: ternary diagrams using ggplot2. J Stat Softw Code Snippets 87(3):1–17. https://doi.org/10.18637/jss.v087.c03

Herzsprung, P., Schultze, M., Hupfer, M., Boehrer, B., Tümpling, W. v., Duffek, A., Van der Veen, A., Friese, K., 2010. Flood effects on phosphorus immobilisation in a river water filled pit lake-Case study Lake Goitsche (Germany). Limnologica 40, 182–190. https://doi.org/10.1016/J.LIMNO.2009.11.007

Horbaczewski, J. K., 2006, "Aluminum precipitation in acidic pit lakes at the Gibbons Creek lignite mine, Texas, USA: Field observations vs. laboratory simulations." p. 785-809. In:

Proceedings of the 7th International Conference on Acid Rock Drainage (ICARD), March 26-30, 2006, St. Louis, MO. R. I. Barnhisel (ed.) Published by the American Society of Mining and Reclamation (ASMR), 3134 Montavesta Road, Lexington, KY 40502.

Hrdinka, T., Šobr, M., Fott, J., Nedbalová, L., 2013. The unique environment of the most acidified permanently meromictic lake in the Czech Republic. Limnologica 43, 417–426. https://doi.org/10.1016/J.LIMNO.2013.01.005

Jia, G., Torri, G., Petruzzi, M., 2004. Distribution coefficients of polonium between 5% TOPO in toluene and aqueous hydrochloric and nitric acids. Appl. Radiat. Isot. 61, 279–282. https://doi.org/10.1016/j.apradiso.2004.03.021

Jiang, M. qin, Jin, X. ying, Lu, X.Q., Chen, Z. liang, 2010. Adsorption of Pb(II), Cd(II), Ni(II) and Cu(II) onto natural kaolinite clay. Desalination 252, 33–39. https://doi.org/10.1016/J.DESAL.2009.11.005

Jones, A.M., Collins, R.N., Rose, J., Waite, T.D., 2009. The effect of silica and natural organic matter on the Fe(II)-catalysed transformation and reactivity of Fe(III) minerals. Geochim. Cosmochim. Acta 73, 4409–4422. https://doi.org/10.1016/J.GCA.2009.04.025

Kleeberg, A., Grüneberg, B., 2005. Phosphorus mobility in sediments of acid mining lakes, Lusatia, Germany. Ecol. Eng. 24, 89–100. https://doi.org/10.1016/J.ECOLENG.2004.12.010

Koźma J., 2009. Rezerwat geologiczno-krajobrazowy Kopalnia Babina w Łęknicy, [in:] Kupetz A., Kupetz M., Der Muskauer Faltenbogen. Wyd. Verlag Dr Freidrich Pfeil, München.

Kupetz M., 1997. Geologischer Bau und Genese der Stauchendmoräne Muskauer Faltenbogen. Branderburgische Geowiss. Beitr., 4: 1–19.

~~Koźma J., Kupetz M., 2008, The transboundary Geopark Muskau Arch, Prz. Geol. 56(8/1): 692–698.~~

Koźma, J., Kupetz, M., 2008. The transboundary Geopark Muskau Arch (Geopark Łuk Mużakowa, Geopark Muskauer Faltenbogen). Przegląd Geol. 56, 692–698.

Labus, K.M., Skoczyńska-Gajda, S., 2013. Origin of sulfates in the post-mining lakes in the eastern part of Muskau Arch (Polish-German borderland). Geol. Q. 57, 561–566. https://doi.org/10.7306/GQ.1110

Lieser, K.H., Steinkopff, T.H., 1989. Chemistry of radioactive cesium in the hydrosphere and in the geosphere. Radiochim. Acta 46, 39–48. https://doi.org/10.1524/RACT.1989.46.1.39

Lutyńska, S., Labus, K., 2015. Identification of processes controlling chemical composition of pit lakes waters located in the eastern part of Muskau Arch (Polish-German borderland). Arch. Environ. Prot. 41, 60–69. https://doi.org/10.1515/aep-2015-0031

Madruga, M.J., Silva, L., Gomes, A.R., Libânio, A., Reis, M., 2014. The influence of particle size on radionuclide activity concentrations in Tejo River sediments. J. Environ. Radioact. 132, 65–72. https://doi.org/10.1016/J.JENVRAD.2014.01.019

Mantero, J., Thomas, R., Holm, E., Rääf, C., Vioque, I., Ruiz-Canovas, C., García-Tenorio, R., Forssell-Aronsson, E., Isaksson, M., 2020. Pit lakes from Southern Sweden: natural radioactivity and elementary characterization. Sci. Rep. 10, 1–17. https://doi.org/10.1038/s41598-020-70521-0

Martin, A., Blanchard, R.L., 1969. The thermal volatilisation of caesium-137, polonium-210 and lead-210 from in vivo labelled samples. Analyst 94, 441–446. https://doi.org/10.1039/AN9699400441

Masbou, J., Viers, J., Grande, J.A., Freydier, R., Zouiten, C., Seyler, P., Pokrovsky, O.S., Behra, P., Dubreuil, B., de la Torre, M.L., 2020. Strong temporal and spatial variation of dissolved Cu isotope composition in acid mine drainage under contrasted hydrological conditions. Environ. Pollut. 266, 115104. https://doi.org/10.1016/J.ENVPOL.2020.115104

Matthews, K.M., Kim, C.K., Martin, P., 2007. Determination of 210Po in environmental materials: A review of analytical methodology. Appl. Radiat. Isot. 65, 267–279. https://doi.org/10.1016/J.APRADISO.2006.09.005

Mayes, W.M., Perks, M.T., Large, A.R.G., Davis, J.E., Gandy, C.J., Orme, P.A.H., Jarvis, A.P., 2021. Effect of an extreme flood event on solute transport and resilience of a mine water treatment system in a mineralised catchment. Sci. Total Environ. 750. https://doi.org/10.1016/J.SCITOTENV.2020.141693

McKinley, J.P., Zeissler, C.J., Zachara, J.M., Jeffrey Serne, R., Lindstrom, R.M., Schaef, H.T., Orr, R.D., 2001. Distribution and retention of ^{137}Cs in sediments at the Hanford Site, Washington. Environ. Sci. Technol. 35, 3433–3441.

Meyers, P.A., Ishiwatari, R., 1995. Organic Matter Accumulation Records in Lake Sediments. Phys. Chem. Lakes 279–328. https://doi.org/10.1007/978-3-642-85132-2_10

MKOO (Międzynarodowa Komisja Ochrony Odry przed Zanieczyszczeniem), 2010. Wezbranie w zlewni Nysy Łużyckiej 7–10 sierpnia 2010 r. (in Polish). Wrocław, Drezno, Praga. http://www.mkoo.pl/download.php?fid=4043&lang=PL

Mukai, H., Hirose, A., Motai, S., Kikuchi, R., Tanoi, K., Nakanishi, T.M., Yaita, T., Kogure, T., 2016. Cesium adsorption/desorption behavior of clay minerals considering actual contamination conditions in Fukushima. https://doi.org/10.1038/srep21543

Naulier, M., Eyrolle-Boyer, F., Boyer, P., Métivier, J.M., Onda, Y., 2017. Particulate organic matter in rivers of Fukushima: An unexpected carrier phase for radiocesiums. Sci. Total Environ. 579, 1560–1571. https://doi.org/10.1016/j.scitotenv.2016.11.165

Nordstrom, D.K., Alpers, C.N., 1999. Geochemistry of acid mine waters. In: Plumlee, G.S., Logsdon, M.J. (Eds.), The Environmental Geochemistry of Mineral Deposits, Part A. Processes, Techniques, and Health Issues. Rev. Econ. Geol. 6A, 133–156.

Nordstrom, D.K., Ball, J.W., 1986. The geochemical behavior of aluminum in acidified surface waters. Science (80-.). 232, 54–56. https://doi.org/10.1126/SCIENCE.232.4746.54

Oszkinis-Golon, M., Frankowski, M., Pukacz, A., 2021. Macrophyte diversity as a response to extreme conditions in the post-mining lakes of the muskau arch (West poland). Water (Switzerland) 13, 2909. https://doi.org/10.3390/W13202909/S1

Paikaray, S., 2020. Environmental Stability of Schwertmannite: A Review. Mine Water Environ. 2020 403 40, 570–586. https://doi.org/10.1007/S10230-020-00734-2

Paikaray, S., Schröder, C., Peiffer, S., 2017. Schwertmannite stability in anoxic Fe(II)-rich aqueous solution. Geochim. Cosmochim. Acta 217, 292–305. https://doi.org/10.1016/J.GCA.2017.08.026

Park, C.W., Kim, S.M., Kim, I., Yoon, I.H., Hwang, J., Kim, J.H., Yang, H.M., Seo, B.K., 2021. Sorption behavior of cesium on silt and clay soil fractions. J. Environ. Radioact. 233, 106592. https://doi.org/10.1016/J.JENVRAD.2021.106592

Park, S.M., Alessi, D.S., Baek, K., 2019. Selective adsorption and irreversible fixation behavior of cesium onto 2:1 layered clay mineral: A mini review. J. Hazard. Mater. 369, 569–576. https://doi.org/10.1016/J.JHAZMAT.2019.02.061

PGW WP (Państwowe Gospodarstwo Wodne Wody Polskie), 2021. MZP (Mapy zagrożenia powodziowego). https://wody.isok.gov.pl/imap_kzgw/?gpmap=gpMZP

Pukacz, A., Oszkinis-Golon, M., Frankowski, M., 2018. The Physico-Chemical Diversity of Pit Lakes of the Muskau Arch (Western Poland) in the Context of Their Evolution and Genesis. Limnol. Rev. 2018, Vol. 18, Pages 115-126 18, 115–126. https://doi.org/10.2478/LIMRE-2018-0013

Pukacz, A., Oszkinis-Golon, M., Frankowski, M., 2020. The physico-chemical diversity of pit lakes of the Muskau Arch (Western Poland) in the context of their evolution and genesis. Limnol. Rev. 18, 115–126. https://doi.org/10.2478/limre-2018-0013

Putyrskaya, V., Klemt, E., Röllin, S., Astner, M., Sahli, H., 2015. Dating of sediments from four Swiss prealpine lakes with ^{210}Pb determined by gamma-spectrometry: Progress and problems. J. Environ. Radioact. 145, 78–94. https://doi.org/10.1016/j.jenvrad.2015.03.028

R Core Team. (2021). R: A language and environment for statistical computing. R Foundation for Statistical Computing, Vienna, Austria. R version 4.0. 4.

Ram, R., Vaughan, J., Etschmann, B., Brugger, J., 2019. The aqueous chemistry of polonium (Po) in environmental and anthropogenic processes. J. Hazard. Mater. 380, 120725. https://doi.org/10.1016/j.jhazmat.2019.06.002

Ramstedt, M., Carlsson, E., Lövgren, L., 2003. Aqueous geochemistry in the Udden pit lake, northern Sweden. Appl. Geochemistry 18, 97–108. https://doi.org/10.1016/S0883-2927(02)00068-9

Rzepa, G., Bożęcki, P., 2007. Mineral composition of AMD precipitates in the Łęknica region (the Muskau Arch, western Poland). XX

Sánchez España, J., López Pamo, E., Santofimia Pastor, E., Reyes Andrés, J., Martín Rubí, J.A., 2006. The removal of dissolved metals by hydroxysulphate precipitates during oxidation and neutralization of acid mine waters, Iberian Pyrite Belt. Aquat. Geochemistry 12, 269–298. https://doi.org/10.1007/S10498-005-6246-7/METRICS

Sánchez España, J., Pamo, E.L., Pastor, E.S., Ercilla, M.D., 2008. The acidic mine pit lakes of the Iberian Pyrite Belt: An approach to their physical limnology and hydrogeochemistry. Appl. Geochemistry 23, 1260–1287. https://doi.org/10.1016/j.apgeochem.2007.12.036

Sánchez España, J.S., Pamo, E.L., Diez, M., Santofimia, E., 2009. Physico-chemical gradients and meromictic stratification in Cueva de la Mora and other acidic pit lakes of the Iberian Pyrite Belt. Mine Water Environ. 28, 15–29. https://doi.org/10.1007/S10230-008-0059-Z/FIGURES/12

Sánchez-España, J., Yusta, I., Burgos, W.D., 2016. Geochemistry of dissolved aluminum at low pH: Hydrobasaluminite formation and interaction with trace metals, silica and microbial cells under anoxic conditions. Chem. Geol. 441, 124–137. https://doi.org/10.1016/J.CHEMGEO.2016.08.004

Sawhney, B.L., 1972. Selective sorption and fixation of cations by clay minerals. A review. Clays Clay Miner. 20, 93–100. https://doi.org/10.1346/CCMN.1972.0200208

Schultze, M., 2013. Limnology of Pit Lakes. Environ. Sci. Eng. 23–224. https://doi.org/10.1007/978-3-642-29384-9_3/TABLES/24

Schultze, M., Boehrer, B., Wendt-Potthoff, K., Katsev, S., Brown, E.T., 2017. Chemical Setting and Biogeochemical Reactions in Meromictic Lakes 35–59. https://doi.org/10.1007/978-3-319-49143-1_3

Schultze, M., Pokrandt, K.H., Hille, W., 2010. Pit lakes of the Central German lignite mining district: Creation, morphometry and water quality aspects. Limnologica 40, 148–155. https://doi.org/10.1016/j.limno.2009.11.006

Schulz, K., Thomasarrigo, L.K., Kaegi, R., Kretzschmar, R., 2022. Stabilization of Ferrihydrite and Lepidocrocite by Silicate during Fe(II)-Catalyzed Mineral Transformation: Impact on Particle Morphology and Silicate Distribution. Environ. Sci. Technol. 56, 5929–5938. https://doi.org/10.1021/ACS.EST.1C08789/ASSET/IMAGES/LARGE/ES1C08789_0005.JPEG

Schwertmann, U., Bigham, J.M., Murad, E., 1995. The first occurrence of schwertmannite in a natural stream environment. Eur. J. Mineral. 7, 547–552. https://doi.org/10.1127/ejm/7/3/0547

~~Sekudewicz, I., Gąsiorowski, M., 2019. Determination of the activity and the average annual dose of absorbed uranium and polonium in drinking water from Warsaw. J. Radioanal. Nucl. Chem. 319, 1351–1358. https://doi.org/10.1007/s10967-018-6351-x~~

Sekudewicz, I., Gąsiorowski, M., 2022. Spatial and vertical distribution of ^{137}Cs activity concentrations in lake sediments of Turawa Lake (Poland). Environ. Sci. Pollut. Res. Int. 29. https://doi.org/10.1007/S11356-022-21417-1

Shepard FP (1954) Nomenclature based on sand-silt-clay ratios. J Sed Pet 24:151–158

Shepard, F.P., 1954. Nomenclature based on sand-silt-clay ratios. J. Sediment. Res. 24, 151–158. https://doi.org/10.1306/D4269774-2B26-11D7-8648000102C1865D

Sienkiewicz, E., Gasiorowski, M., 2016. The evolution of a mining lake - From acidity to natural neutralization. Sci. Total Environ. 557–558, 343–354. https://doi.org/10.1016/j.scitotenv.2016.03.088

Sienkiewicz, E., Gąsiorowski, M., 2018. The influence of acid mine drainage on the phytoand zooplankton communities in a clay pit lake in the ŁUK Muzakowa Geopark (western Poland). Fundam. Appl. Limnol. 191, 143–154. https://doi.org/10.1127/FAL/2018/1079

Smith, K.S., 1999. Metal sorption on mineral surfaces: an overview with examples relating to mineral deposits. In: Plumlee, G.S., Losdon, M.J. (Eds.), The Environmental Geochemistry of Mineral Deposits, Part A. Processes, Techniques, and Health Issues: Society of Economic Geologists, Rev. Econ. Geol. 6A, pp. 161–182.

Solski, A., Jędrczak, A., & Matejczuk, W. (1988). Skład chemiczny wód zbiorników pojezierza antropogenicznego w rejonie Tuplice-Łęknica (in Polish). Zeszyty Naukowe Uniwersytetu Zielonogórskiego, 84, 65–76.

Somboon, S., Kavasi, N., Sahoo, S.K., Inoue, K., Arae, H., Tsuruoka, H., Shimizu, H., Fukushi, M., 2018. Radiocesium and 40K distribution of river sediments and floodplain deposits in the Fukushima exclusion zone. J. Environ. Radioact. 195, 40–53. https://doi.org/10.1016/j.jenvrad.2018.09.003

Stewart, G., Kirk Cochran, J., Xue, J., Lee, C., Wakeham, S.G., Armstrong, R.A., Masqué, P., Carlos Miquel, J., 2007. Exploring the connection between ^{210}Po and organic matter in the northwestern Mediterranean. Deep Sea Res. Part I Oceanogr. Res. Pap. 54, 415–427. https://doi.org/10.1016/J.DSR.2006.12.006

Stumm, W., Morgan, J.J., 1996. Aquatic Chemistry. John Wiley & Sons, New York.

Swarzenski, P.W., 2014. ^{210}Pb Dating, in: Encyclopedia of Scientific Dating Methods. Springer Netherlands, Dordrecht, pp. 1–11. https://doi.org/10.1007/978-94-007-6326-5_236-1

Thomas, R.I., Mantero, J.I., Ruiz Cá novas, C.I., Holm, E., García-Tenorio, R., Forssell-AronssonID, E., IsakssonID, M., 2022. Natural radioactivity and element characterization in pit lakes in Northern Sweden. https://doi.org/10.1371/journal.pone.0266002

Thurman, E.M., 1985. Organic geochemistry of natural waters, Martinus Nijhoff/Dr. W. Junk Publishers, Dordrecht.

Torres, E., Ayora, C., Canovas, C.R., García-Robledo, E., Galván, L., Sarmiento, A.M., 2013. Metal cycling during sediment early diagenesis in a water reservoir affected by acid mine drainage. Sci. Total Environ. 416–429. https://doi.org/10.1016/j.scitotenv.2013.05.014

Vink, J.P.M., Harmsen, J., Rijnaarts, H., 2010. Delayed immobilization of heavy metals in soils and sediments under reducing and anaerobic conditions; consequences for flooding and storage. J. Soils Sediments 10, 1633–1645. https://doi.org/10.1007/S11368-010-0296-1/FIGURES/4

Vithana, C.L., Sullivan, L.A., Burton, E.D., Bush, R.T., 2015. Stability of schwertmannite and jarosite in an acidic landscape: Prolonged field incubation. Geoderma 239, 47–57. https://doi.org/10.1016/J.GEODERMA.2014.09.022

Walling, D E, Quine, T.A., 1993. Use of caesium-137 as a tracer of erosion and sedimentation: Handbook for the application of the caesium-137 technique. UK Overseas Dev. Adm. Res. Scheme R 4579.

Wisotzky, F., 1998. Chemical Reactions in Aquifers Influenced by Sulfide Oxidation and in Sulfide Oxidation Zones. Acidic Min. Lakes 223–236. https://doi.org/10.1007/978-3-642-71954-7_11

Zapata, F., Nguyen, M.L., 2009. Chapter 7 Soil Erosion and Sedimentation Studies Using Environmental Radionuclides. Radioact. Environ. 16, 295–322. https://doi.org/10.1016/S1569-4860(09)01607-6

Figure captions

Table 1 Physicochemical parameters of surface (T) and lake waters (WA and WB) in Lake ŁK-61 in the Mushau Arch. Sampling sites are shown in Fig. 1.

Fig. 1. Sampling site with (A) flood hazard map MZP 10% (once per 10 years) (PGW WP, 2021; modified) and (B) bathymetric map of ŁK-61 Lake.

Fig. 2. Geological setting of ŁK-61 Lake. The geological data are based on the Detailed Geological Map of Poland (Bartczak and Gancarz, 2001).

Fig. 3.

Fig. 4.

Fig. 5. XRD spectra of selected samples of lake sediments collected from (A) 5 cm and (B) 10 cm depth of the core of ŁK-61 lake.

Fig. 6. IR spectra (A) of selected samples of lake sediments collected from particular depths and (B) from 10 cm depth of the core of ŁK-61 Lake.

Fig. 7. Chemical composition of iron oxyhydroxides from samples of lake sediments collected from the depths of 5 cm (A), 7 cm (B), 9 cm (C), and 50 cm (D) of the core.

Fig. 8. Different types of iron oxyhydroxides form ŁK-61 lake.

Table 1 Physicochemical parameters of tributary (T) and lake waters (WA and WB) of ŁK-61 Lake in the Muskau Arch. Sampling sites are shown in Fig. 1.

	Bożęcki (2013)			**Water column**							**Tributary**			**Water column**		
Sample name				WA1	WA2	WA3	WA4	WA5	WA6	WA7	T1	T2	T3	WB1	WB2	WB3
Sampling date	09/2009	08/2010	09/2010	09/2020							09/2020			09/2021		
Depth (m)	surface			0.5	1.5	2.5	3.5	4.5	5.5	6.5	surface			0.5	6.5	7.5
Temperature (°C)	16.3	20.3	16.7	19.3	18.5	18.3	18.2	18.2	17.7	14.7	18.7	14.0	14.4	19.6	13.7	12.5
pH	2.9	5.3	3.9	2.85	2.88	2.86	2.87	2.86	2.86	5.98	2.80	3.09	3.14	2.9	3.2	6.5
Eh (mV)	765	555	666	540	541	543	544	544	540	-22	532	449	432	541	410	-105
Conductivity (µS/cm)	1856	268	593	1964	1975	1995	1989	2001	2001	2780	1964	1892	1849	1908	2100	2330
Dissolved oxygen (mg/L)	n.d.	n.d.	n.d.	9.25	9.33	9.38	9.41	9.33	9.21	1.60	9.13	8.78	8.70	9.00	4.35	1.83

n.d. – not detected

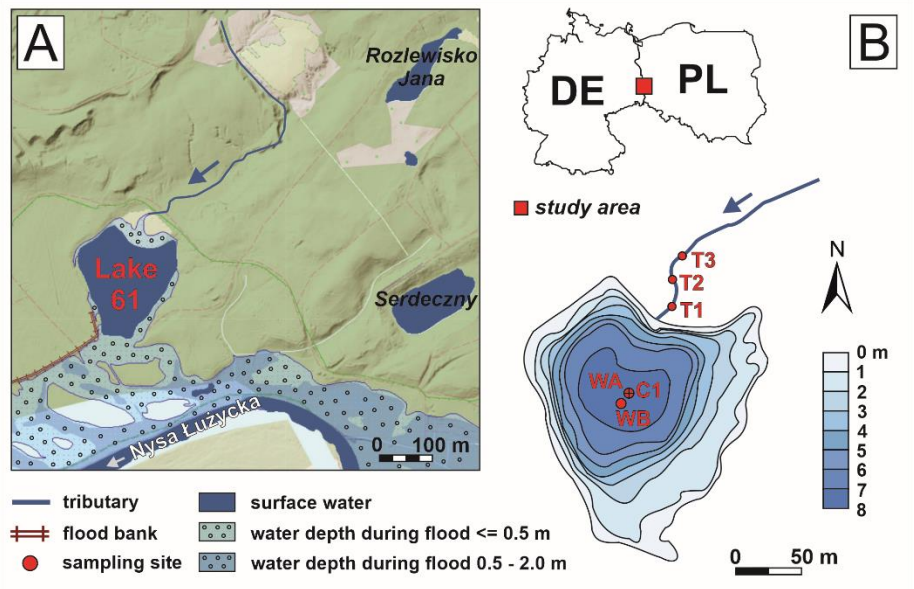

Fig. 1. Sampling site with (A) flood hazard map MZP 10% (once per 10 years) (PGW WP, 2021; modified) and (B) bathymetric map of ŁK-61 Lake.

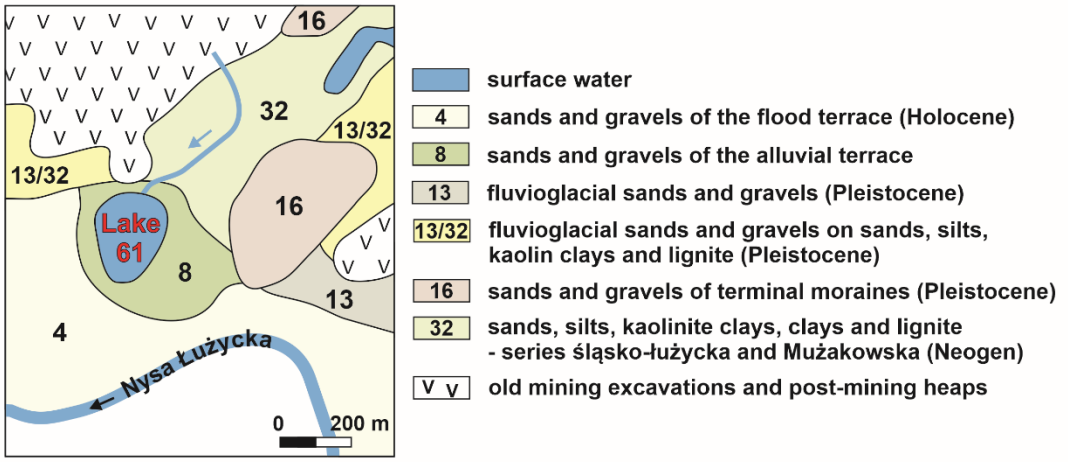

Fig. 2. Geological setting of ŁK-61 Lake. The geological data are based on the Detailed Geological Map of Poland (Bartczak and Gancarz, 2001).

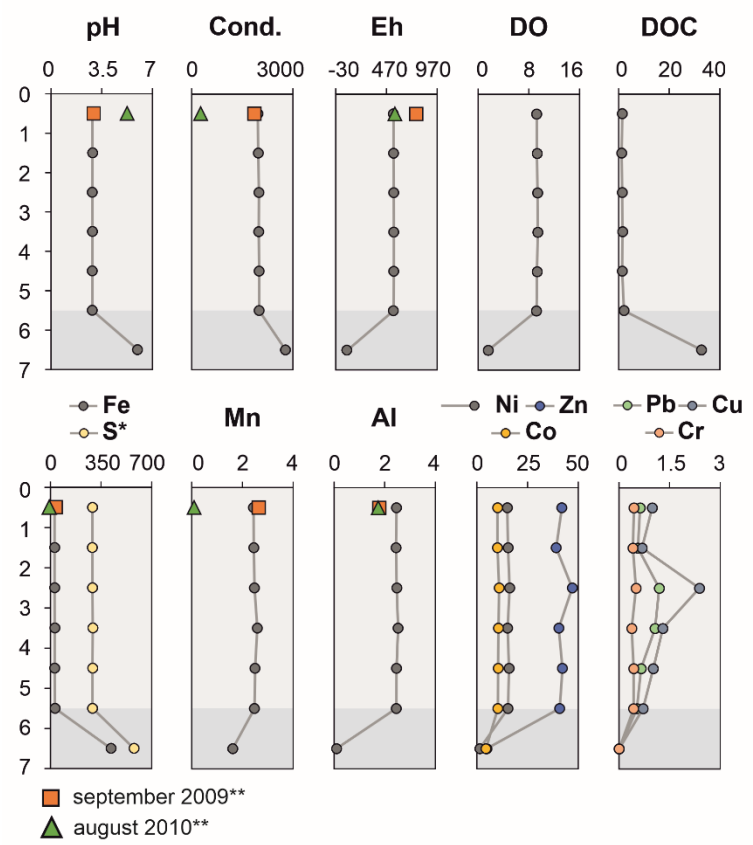

Fig. 3 The vertical distribution of the selected psychochemical parameters (pH, Cond. – conductivity (µS/cm), Eh (mV)), and the content of DO, DOC, Fe, S, Mn, Al (mg/L) and Ni, Zn, Co, Pb, Cu, Cr (µg/L) in the water column of ŁK-61 Lake. * – data from Bożęcki (2013) not presented for S; ** – values measured by Bożęcki (2013)

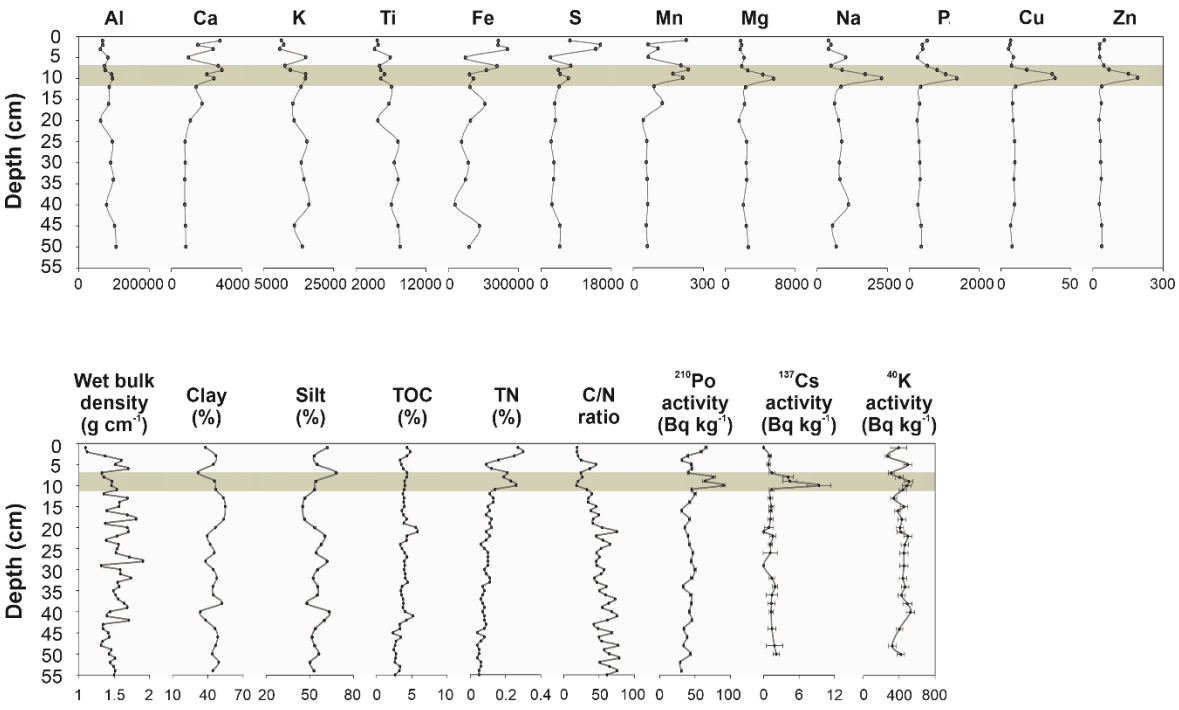
Al
Ca
K
Ti
Fe
S
Mn
Mg
Na
P
Cu
Zn
Depth (cm)
Wet bulk density (g cm-1)
Clay (%)
Silt (%)
TOC (%)
TN (%)
C/N ratio
210Po activity (Bq kg-1)
137Cs activity (Bq kg-1)
40K activity (Bq kg-1)

Fig. 4.

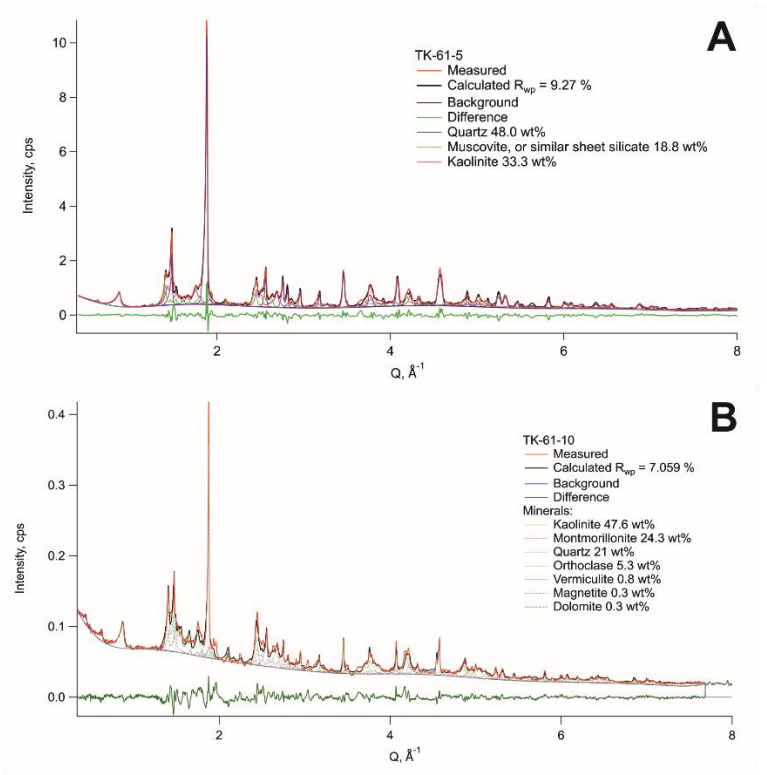

Fig. 5. XRD spectra of selected samples of lake sediments collected from (A) 5 cm and (B) 10 cm depth of the core of ŁK-61 lake.

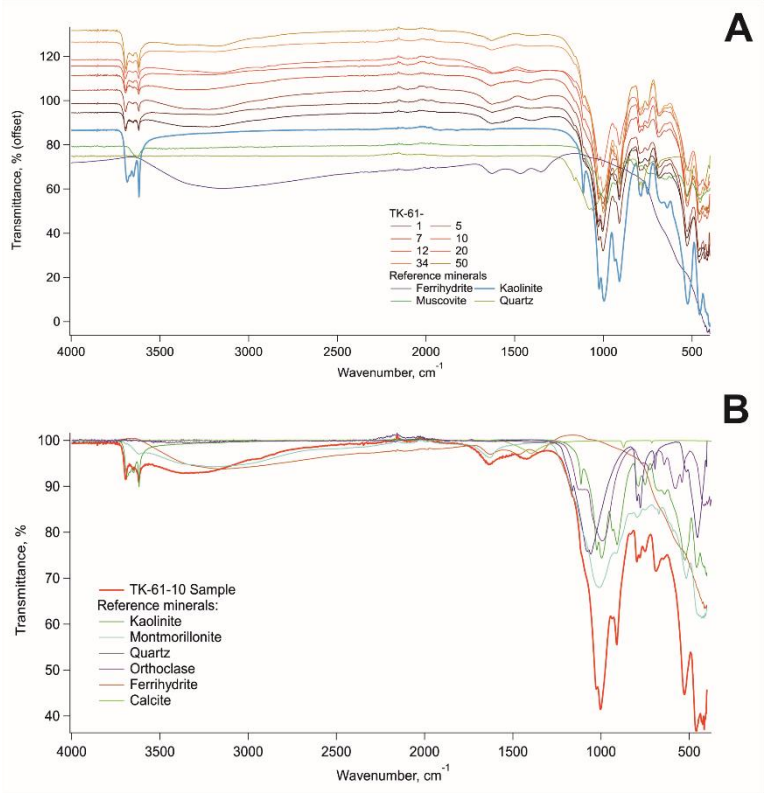

Fig. 6. IR spectra (A) of selected samples of lake sediments collected from particular depths and (B) from 10 cm depth of the core of ŁK-61 Lake.

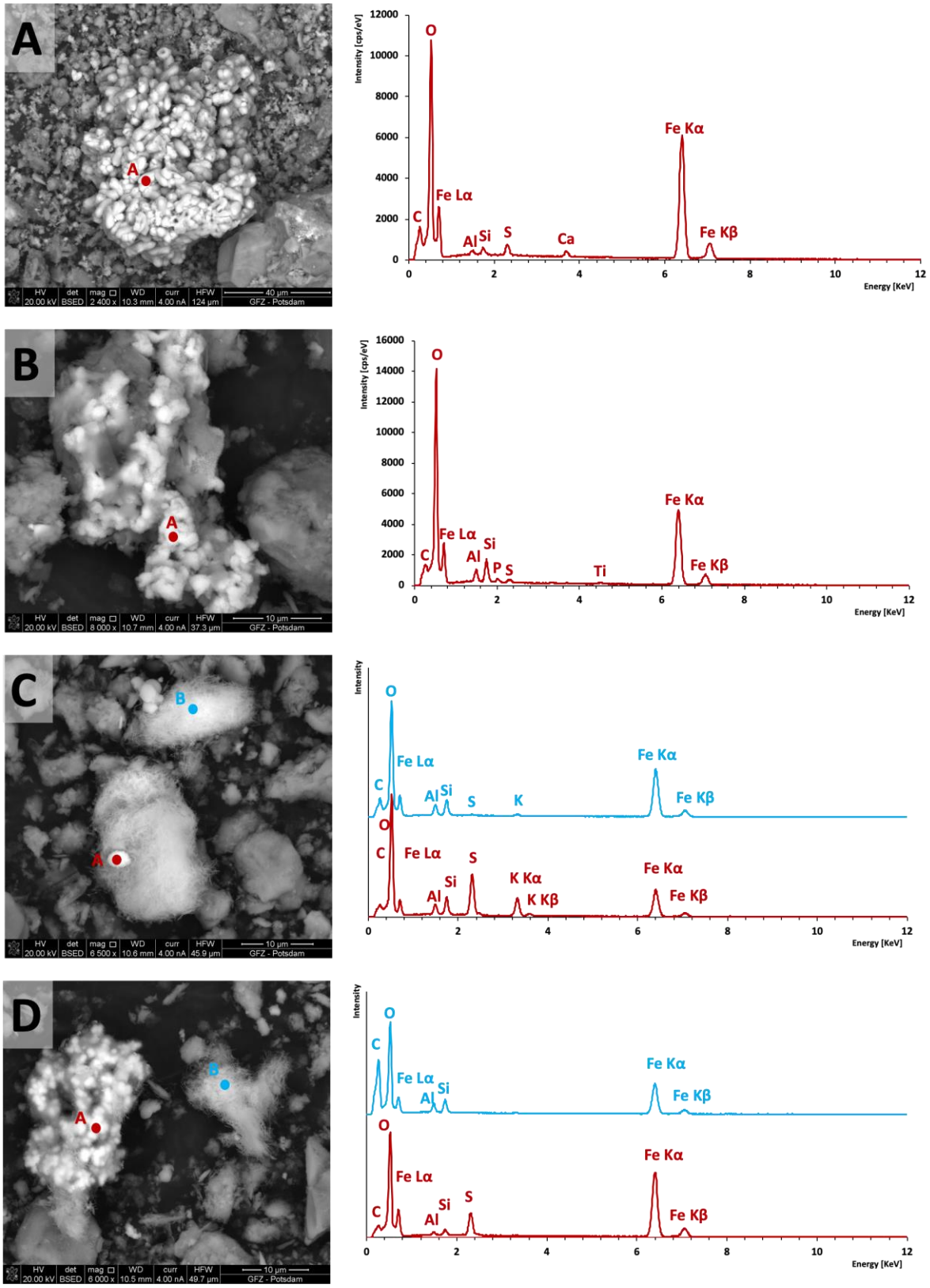

Fig. 7. Chemical composition of iron oxyhydroxides from samples of lake sediments collected from the depths of 5 cm (A), 7 cm (B), 9 cm (C), and 50 cm (D) of the core.

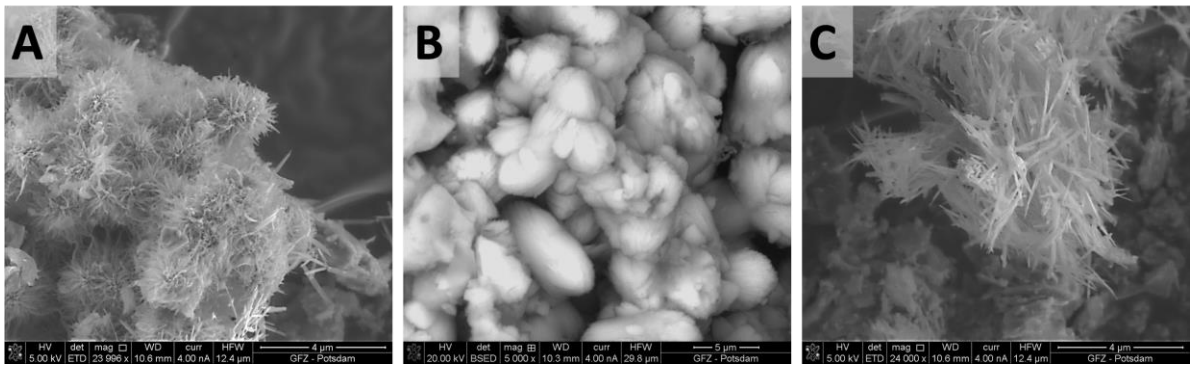

Fig. 8. Different types of iron oxyhydroxides form ŁK-61 lake.